DOT/TSC-241-4

Project Report
ATC-26, Vol. I

Technical Assessment of Satellites for CONUS Air Traffic Control, Volume I: Coordinated Aircraft-to-Satellite Techniques

R.S. Orr
K.S. Schneider

31 January 1974

Lincoln Laboratory
MASSACHUSETTS INSTITUTE OF TECHNOLOGY
LEXINGTON, MASSACHUSETTS

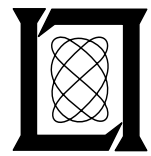

Prepared for the Transportation Systems Center.

TECHNICAL REPORT STANDARD TITLE PAGE

1. Report No.	2. Government Accession No.	3. Recipient's Catalog No.
DOT/TSC-241-4		

4. Title and Subtitle	5. Report Date
Technical Assessment of Satellites for CONUS Air Traffic Control Vol. I: Coordinated Aircraft-to-Satellite Techniques	31 January 1974
	6. Performing Organization Code

7. Author(s)	8. Performing Organization Report No.
R. S. Orr and K. S. Schneider	ATC-26, Vol. I

9. Performing Organization Name and Address	10. Work Unit No.
Massachusetts Institute of Technology Lincoln Laboratory P. O. Box 73 Lexington, Massachusetts 02173	11. Contract or Grant No. DOT/TSC-241
	13. Type of Report and Period Covered Project Report
12. Sponsoring Agency Name and Address Transportation Systems Center Department of Transportation Cambridge, Massachusetts	14. Sponsoring Agency Code

15. Supplementary Notes

The work reported in this document was performed at Lincoln Laboratory, a center for research operated by Massachusetts Institute of Technology.

16. Abstract

A number of satellite system techniques have been suggested as candidates to provide ATC surveillance, communication, and/or navigation service over CONUS. All techniques perform position determination by multilateration using a constellation of satellites. They can be categorized as follows: 1) Coordinated Aircraft-to-Satellite Techniques (CAST), 2) Random Access Aircraft-to-Satellite Techniques (RAST), and 3) Satellite-to-Aircraft Techniques (SAT). A technical assessment is made of the various techniques with no one particular technique emerging as superior; several feasible alternatives are identified. The assessment indicates that satellite based techniques for CONUS ATC can be developed without relying on high risk technology.

This volume deals with CAST; RAST and SAT are treated in companion volumes. A system employing CAST could operate by having each aircraft transmit only in response to an interrogation from a satellite. The position of the aircraft is then obtained by multilateration using the arrival times of its response at four or more satellites. A digital message can accompany each interrogation or response. By properly coordinating the interrogations, mutual interference between different response can be avoided. The critical technical aspects of CAST are explored with special emphasis on signaling formats, avionics, the satellite antenna and susceptibility to jamming.

17. Key Words	18. Distribution Statement
Air Traffic Control surveillance satellite systems AATMS	Document is available to the public through the National Technical Information Service, Springfield, Virginia 22151.

19. Security Classif. (of this report)	20. Security Classif. (of this page)	21. No. of Pages	22. Price
Unclassified	Unclassified	132	4.50 HC 1.45 MF

Form DOT F 1700.7 (8-69)

CONTENTS

CONTENTS (Continued)

CONTENTS (Continued)

CONTENTS (Continued)

LIST OF ILLUSTRATIONS

LIST OF ILLUSTRATIONS (Continued)

LIST OF TABLES

LIST OF TABLES (Continued)

SECTION 1

INTRODUCTION AND SUMMARY OF CONCLUSIONS

1.1 OVERVIEW OF SATELLITE SYSTEM TECHNIQUES

Over the last half decade, a number of satellite system techniques have been advanced as candidates to provide Air Traffic Control (ATC) surveillance, communication and/or navigation service over the CONtinental United States (CONUS) [1-7]. Each technique has its advantages and disadvantages. All employ position determination service by multilateration using a constellation of satellites. These techniques can be grouped into three basic categories based on certain key technical features. The three categories are:

Coordinated Aircraft-to-Satellite Techniques (CAST)

Systems employing these techniques interrogate aircraft sequentially. The response from an aircraft is the transmission of a timing pulse. This pulse is received by the satellites and then relayed to a ground processing facility. The ground processing facility determines the signal time of arrival (TOA) at each of the satellites and estimates the aircraft position by multilateration. The position information is then incorporated into the ATC surveillance data base. The interrogation algorithm is designed to eliminate overlapping signal pulses at the satellites and hence mutual interference.

Random Access Aircraft-to-Satellite Techniques (RAST)

Systems employing these techniques have each aircraft transmit a timing pulse which is received by four or more satellites and relayed to a ground processing facility. This facility determines TOA at each of the satellites and estimates the aircraft position by hyperbolic multilateration. The position information is then incorporated into the ATC surveillance data base. Since aircraft transmit in an uncoordinated manner, system performance, i.e., accuracy and update rate, is ultimately limited by mutual interference caused by signal overlap at satellite receivers.

Satellite-to-Aircraft Techniques (SAT)

Systems employing these techniques operate by having four or more satellites periodically transmit timing pulses to aircraft. A navigation processor (computer) aboard each aircraft determines the aircraft position form the signal TOA's. The information also can be data linked to the ground for inclusion in a ground maintained ATC surveillance data base.

This volume is concerned with an assessment of the critical technical aspects of Coordinated Aircraft-to-Satellite Techniques (CAST). The other two techniques are treated in Volumes II and III [8, 9].

These three volumes concentrate only on the crucial technical issues. They do not attempt to assess the broad spectrum of operational or economic implications of employing these techniques in the National Airspace System. Issues such as the cost-effectiveness of satellites as an element in the CONUS ATC system are beyond the scope of these investigations. Detailed questions concerning the manner by which any of these satellite techniques might evolve from present day aircraft surveillance/navigation systems are also outside the scope of this report. Detailed operational requirements that would be imposed upon a satellite system for CONUS ATC have not been given consideration in depth.

The results of the technical assessment of all three satellite techniques have verified that satellite-based techniques for CONUS ATC could be developed without reliance on high risk technology. No one particular technique has emerged as superior; rather, several feasible alternatives have been identified.

One of the primary attractive attributes of satellites is their inherent ability to provide broad coverage of low altitude airspace. Unpressurized general aviation aircraft are predominant users of low altitude airspace.

Hence, a central issue is the complexity of general aviation avionics required for satellite operation. It has been concluded that all three of the techniques considered require more complex avionics (for a given user class) than is currently employed for comparable service with today's ground based system.

1.2 COORDINATED AIRCRAFT-TO-SATELLITE TECHNIQUES (CAST)

The techniques considered in this volume employ a constellation of synchronous satellites. Each participating aircraft requires a transponder for surveillance (and digital communication). A feature which distinguishes these techniques from the others is the required presence of both a digital interrogation downlink between at least one satellite and participating aircraft and a digital uplink between participating aircraft and the satellites in the constellation.

CAST operates as follows. An interrogation satellite transmits a signal to a given aircraft over the interrogation downlink; this signal is received by the intended aircraft, and a reply is elicited which is received over the uplink at all the visible satellites in the constellation. These replies are relayed to one (or more) ground stations at which the signal times of arrival are measured. These times of arrival are used in conjunction with a multilateration technique to estimate the position of the aircraft. Digital messages may be transmitted along with the interrogation and reply signals. This procedure is repeated periodically for each user aircraft in order to have continually updated surveillance. By careful selection of the interrogation algorithm CAST avoids the performance degradation found in RAST [1, 10] (due to possible overlap signals from multiple aircraft).

1.3 SUMMARY OF PRINCIPAL CONCLUSIONS

As a result of the study reported herein, a number of conclusions can be drawn. These conclusions pertain principally to the technological feasibility of CAST and the preferred alternatives in system realizations.

A. NO IMPENETRABLE TECHNOLOGICAL BARRIERS PRECLUDE THE FEASIBILITY OF EMPLOYING COORDINATED AIR-TO-SATELLITE TECHNIQUES.

The satellite and avionics technologies which are pertinent to these techniques appear to be well within present day capabilities. Consequently, the feasibility is not contingent upon any high risk technological advance.

B. HIGH GAIN SATELLITE ANTENNAS ARE DICTATED BY THE DESIRE FOR LOW COST AVIONICS WHICH ARISES FROM THE INCLUSION OF GENERAL AVIATION IN THE SYSTEM.

Among the numerous alternatives for the realization of a position determination system, certain ones are strongly preferred with regard to the inclusion of general aviation aircraft with low cost avionics. Specifically, by employing a large, high gain, narrow beamwidth antenna rather than a small, moderate gain, CONUS coverage antenna for each satellite, the need for high peak output power and low receiver front end noise figure at the transponder is somewhat diminished. Such an antenna must utilize several beams in order to maintain CONUS coverage. Since coverage regions are neither mutually exclusive nor identical from different satellite positions, care must be exercised in exploiting this capability.

C. THE REQUIRED AVIONICS COMPLEMENT IS SIGNIFICANTLY MORE COMPLEX (AND COSTLY TODAY) THAN THE CORRESPONDING ATCRBS AVIONICS.

Despite the inclusion of high gain satellite antennas, there remain several avionics features which are highly desirable to include but at the same time more expensive than their counterparts in an ATCRBS transponder. The required avionics receiver is more expensive because of the low front end noise temperature. The use of a moderate power coherent avionics transmitter for satisfying the uplink ranging accuracy requirement is significantly more costly.

D. COMMONALITY OF EQUIPMENT WITH UPGRADED THIRD GENERATION ATC AVIONICS CANNOT SUPPORT SUBSTANTIAL SAVINGS IN THE TOTAL AVIONICS COST.

Total avionics cost could in principle be decreased by exploiting commonality among onboard equipment. However, the necessity for upper-hemispherical coverage, operation in the 1535-1660 MHz allocation and coherent transmission provide little opportunity for appreciable savings through integration with other avionics planned for the Upgraded Third Generation System.

E. A LARGE CENTRALIZED DATA PROCESSING FACILITY REQUIRING THE COORDINATED EFFORTS OF SEVERAL TENS OF PRESENT DAY GENERAL PURPOSE CPU'S AND FAST RANDOM ACCESS STORAGE IS NEEDED TO CONTROL THE SYSTEM. RELIABLE HARDWARE AND SOFTWARE ENGINEERING FOR SUCH A FACILITY IS A DIFFICULT BUT FEASIBLE GOAL.

The data rates at the ground in this type of system are such that a large amount of simultaneous processing is required for position determination, communication processing and interrogation scheduling. Rapid random

access (possibly precluding disc and drum storage) to aircraft track files is also required for efficient interrogation. All told, these processing requirements are more demanding than those of, for example, NAS Stage A.

F. CAST SYSTEMS ARE VULNERABLE TO FAILURE OF THEIR CENTRAL PROCESSING FACILITY AND TO THREATS FROM A TERRESTRIAL JAMMER.

The facility required to execute the computational functions must be centralized. As such, operation of the entire system is sensitive to failure of this facility. The aircraft-to-satellite link is vulnerable to threats from terrestrial jammers. Several jammers appropriately located in CONUS could disable an entire CAST system using very inexpensive technology.

G. CAST CAN BE DESIGNED TO HAVE A CAPACITY* AT LEAST SUFFICIENT TO PROVIDE SERVICE TO AIRCRAFT IN THE EN ROUTE ENVIRONMENT, OR TO THOSE OUTSIDE THE COVERAGE OF A GROUND BASED SYSTEM.

The basis of this observation is found in the following subsection, in which representative CAST system characteristics are presented based upon the work in this volume. The estimated capacity of 30,000 aircraft is consistent with the services described above.

1.4 REPRESENTATIVE CAST SYSTEM CHARACTERISTICS

The results of the performance analyses in Volume I are summarized here in the presentation of a representative CAST system. Tables 1.1-1.3 summarize its significant features.

*Average number of aircraft serviced.

Table 1.1. System Services.

Capacity	30,000 aircraft
Position Update Period (average)	10 sec
Surveillance Accuracy	120-300 ft (rms)
Uplink Data Rate (average)	20 bits/10 sec
Downlink Data Rate (average)	20 bits/10 sec

Table 1.2. Representative Downlink Characteristics.

Modulation - Binary DPSK

Peak Transmitted Power - 1 kW

Transponder Front End Noise Figure - 11 dB

Downlink Signal Format

- Synchronization Signal - Transmitted every 5 msec
- Discrete Aircraft Address
- Communication Message

Address Transmitted by a 31 bit Codeword

Address Chip Duration - 2.50 μsec

Synchronization Signal - 31 bit Maximal Length Sequence

Synchronization Chip Duration - 1.25 μsec

Table 1.3. Representative Uplink Characteristics.

Modulation - Binary DPSK

Peak Transmitter Power - 500 W

Uplink Signal Format

Ranging Signal

Communication Message

Ranging Signal - 85 bit Sequence

Ranging Chip Duration - 100 nsec

Address and Communication Chip Duration - 3.75 μsec

1.5 PROGRAM OF VOLUME I

Our examination of CAST will be carried out using the following program.

We begin in Section 2 with a detailed description of the operation of a system employing CAST. The methods by which the system executes its surveillance and communication functions are discussed in detail. The signal formats used on the aircraft-to-satellite and satellite-to-aircraft links will be described. The interrogation algorithm used to coordinate aircraft transmissions is also described in the section.

The analysis of a CAST system requires an understanding of satellite constellations, satellite antennas and avionics for participating aircraft. Rather than discuss these issues where they arise in context, we choose to discuss them in detail in Section 3, before system performance is examined.

Several of these issues are relevant not only to the CAST, but also to RAST and SAT.

A performance measure for the CAST system is introduced in Section 4; this measure is the capacity of the system, i.e., the number of aircraft it can service. Computation of the capacity requires the satellite-to-aircraft and aircraft-to-satellite link signal-to-noise ratios. These ratios are computed from the representative link power budgets provided in Section 4.

In Section 5 the performance of the satellite-to-aircraft downlink is examined by determining its service capacity. This capacity is a function of the way in which the downlink signaling is executed, i.e., the choice of modulation and coding. The signaling alternatives considered in examining downlink performance are presented in this section before performance is computed.

Section 6 deals with the performance of the aircraft-to-satellite uplink. The capacity of this link is determined. As with the downlink, this capacity is a function of the way in which the signaling is executed, i.e., the choice of modulation and uplink ranging signal. The signaling alternatives considered are presented before performance is computed.

In the final section of this volume, two remaining issues which are critical to the assessment of CAST are examined. These are the susceptibility to intentional jamming and the complexity of the computation required at the ground facility.

SECTION 2

SYSTEM DESCRIPTION AND FEATURES

In this section, typical operation of a system employing CAST is described. The issues to be studied in the remainder of this report are brought out in the course of this discussion.

2.1 SYSTEM ELEMENTS

The pictorial in Figure 2.1 indicates the three major elements for CAST; a constellation of satellites, the participating aircraft, and one or more ground stations. The satellites serve to relay transmissions from the ground station to the aircraft and vice versa. At least one satellite has the capability to transmit to user aircraft so that it can function as an interrogator. All satellites are equipped to receive transmissions from aircraft. In order to satisfy the requirements of a hyperbolic multilateration method of aircraft position determination it will be assumed that at least four satellites are visible from all of CONUS at any time.*

Each participating aircraft carries a transponder allowing it to receive transmissions from the interrogator and to transmit to all satellites. Each aircraft is assigned a unique discrete address by which it is identified.

*In this context, "visible" means that the satellites appear at a sufficiently high elevation angle relative to the plane of the aircraft to insure a sufficiently high received signal level.

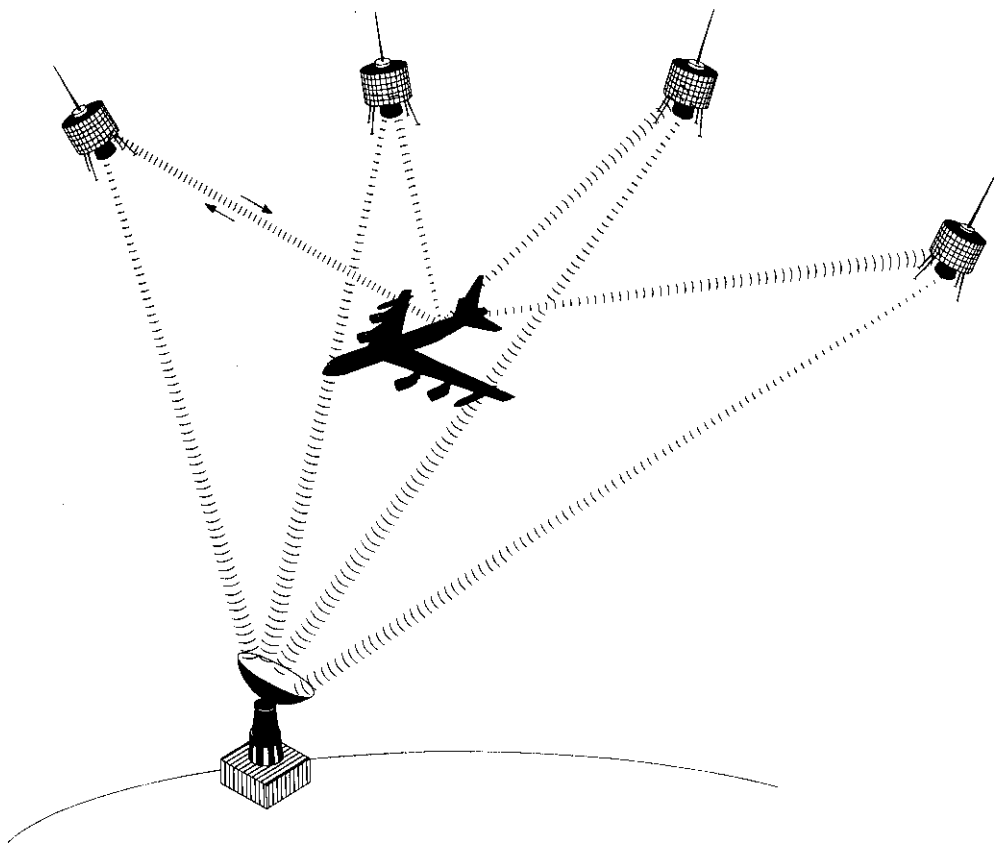

Figure 2.1. ATC Surveillance System Employing CAST.

The ground station schedules the interrogations and transmits the schedule to the interrogator by a ground-to-satellite link. All aircraft replies received by satellites are relayed to the ground station where aircraft positions are computed. A highly automated computational facility is required at the ground station both to schedule interrogations and compute positions.

2.2 SYSTEM DESCRIPTION

It is convenient to identify two primary subsystems; acquisition and interrogation. The acquisition subsystem has as its principal function the detection and initial location of aircraft in the airspace. Aircraft so detected are compiled into a roll and passed on to the interrogation subsystem for accurate position determination and communication. Individual aircraft are discretely interrogated by the interrogation subsystem. The aircraft reply enables the system to compute the position of the aircraft.

Descriptions of the operation of these two subsystems are given below. The discussion of acquisition will be brief since this topic has been investigated elsewhere [2]. The role of the interrogation subsystem, in which the essential system functions take place, is emphasized in the remainder of the report.

2.2.1 Acquisition Subsystem

In the acquisition subsystem, a roll is compiled consisting of the identity (discrete address) and current position of all aircraft to be serviced. This can be accomplished by a variety of methods. Some methods for obtaining acquisition use data obtained by hand-off from some external source. This

source might be a companion surveillance system (e.g., DABS/ATCRBS). Other methods allow the system to accomplish acquisition with complete independence.

As an example [2] of the latter method, one might append to the discrete address of each aircraft additional bits which are used to divide the aircraft into address groups. Acquisition is initiated by the transmission (from the interrogator satellite) of a signal requesting all aircraft within the interrogation beam and belonging to a specific address group to reply with their discrete address. In the referenced example, four such groups are used.

The aircraft roll that is determined during acquisition functions as an input to an interrogation subsystem scheduling algorithm.

The acquisition subsystem is entered when the system is starting up or after a system failure. It must be entered periodically to bring new users into the system.

2.2.2 Interrogation Subsystem

Once an aircraft roll is established by the acquisition subsystem, it is supplied to the interrogation subsystem. An interrogation cycle consists of a sequence of transmissions from the interrogator satellite to different user aircraft and the reception of the resulting aircraft replies by all the visible satellites in the constellation. The order in which aircraft are interrogated is determined anew for each cycle from the previous position (and possibly velocity) estimates.

The operation of the interrogation subsystem can be explained by considering the interrogation of a single aircraft. The signal transmitted to a given aircraft consists of a pair of digital messages. The first is the aircraft's unique address; the second is a binary coded communication message which might, for example, represent an IPC command being relayed from the ground.

The aircraft transponder receives the entire sequence of interrogations and examines the address portion of each. Further action is taken only when it recognizes its own address. When this occurs, the aircraft transponder decodes any included downlink message for display in the cockpit and responds with an uplink waveform containing a ranging signal (for accurate uplink TOA measurements) and an uplink message which might include the aircraft address.

By measuring the arrival times of the ranging signal at all visible satellites the aircraft's position can be estimated. This can be done by a variety of multilateration techniques. For example, elliptical multilateration can be used if the time of interrogation is known and the turn around delay through the aircraft transponder can be estimated with sufficient accuracy. As the uncertainty in turn around delay increases, the optimum elliptical multilateration algorithm can be shown to approach a hyperbolic scheme, in which only arrival time differences are used for the position estimate [11]. Turn around delay plays no part in the accuracy of the hyperbolic estimate.

The computed position of the aircraft is smoothed with previous position data and entered into the aircraft roll, replacing the previous position estimate. Assurance that the newly computed position is associated with the

correct aircraft can be established directly from the interrogation schedule, since overlapping replies have been eliminated.

The sequence of interrogations could be transmitted in strict time serial fashion. Instead, it is assumed that the satellites employ multiple transmitters and a multiple beam antenna, and that interrogation of different aircraft can be executed simultaneously on several different beams. This simultaneity is intended to enlarge the number of users which the system can accommodate. However, these simultaneous interrogations should be carried out without introducing any mutually interfering replies at the receivers. This objective can be achieved using a single downlink frequency and a single uplink frequency if the several antenna beams which transmit (or receive) simultaneously have essentially disjoint coverage footprints on CONUS. As a result, undesired out-of-beam replies will arrive at greatly diminished gain relative to the desired replies.

This approach to the elimination of mutual interference requires that the antenna beams have well separated boresight points and sufficiently narrow beamwidths. The latter requirement in turn implies that the antennas have sufficiently large apertures. Multiple receivers are required at the satellites as well.

The aircraft receiver cannot properly decode the interrogation signals unless it is synchronized to the downlink transmissions. There are many methods by which synchronization could be achieved. We assume that, in CAST, synchronization information is derived from an additional signal transmitted by the interrogator which precedes the interrogation. This synchronization need not, however, be established on an individual basis for each aircraft.

All aircraft can be synchronized by the transmission of a single digital sequence whose time of arrival is measured at the aircraft and is used to set a clock. The interrogations follow at fixed delays relative to the synchronization signal so that the transponder can locate them for demodulation and processing. The synchronization signal is repeated periodically to prevent timing errors due to relative motion and clock instability from degrading the link reliability to an unacceptably low level.

Figure 2.2 illustrates the signal format for both the satellite-to-aircraft downlink and the aircraft-to-satellite uplink over the duration of a single resynchronization period. This format is repeated periodically until interrogation is interrupted. An interrupt will occur at the completion of a cycle of interrogations, and it will occur several times prior to that since the interrogator satellite is assumed to operate in half duplex mode.* Only a few hundred milliseconds of interrogation can be transmitted before a listening interrupt must occur. The pattern of interrogation and interrupt continues until all aircraft on the roll have been interrogated.

2.2.3 Interrogation Scheduling

A primary motivation for considering CAST is the elimination of the mutual interference problem which plagues systems employing RAST [1, 10]. Since all users share a common uplink frequency, this objective is met by careful coordination in time of the uplink replies.

*In half duplex mode, the satellite does not transmit and receive simultaneously. A full duplex (simultaneous T/R) interrogator would lead to more efficient channel usage, but at increased equipment expense.

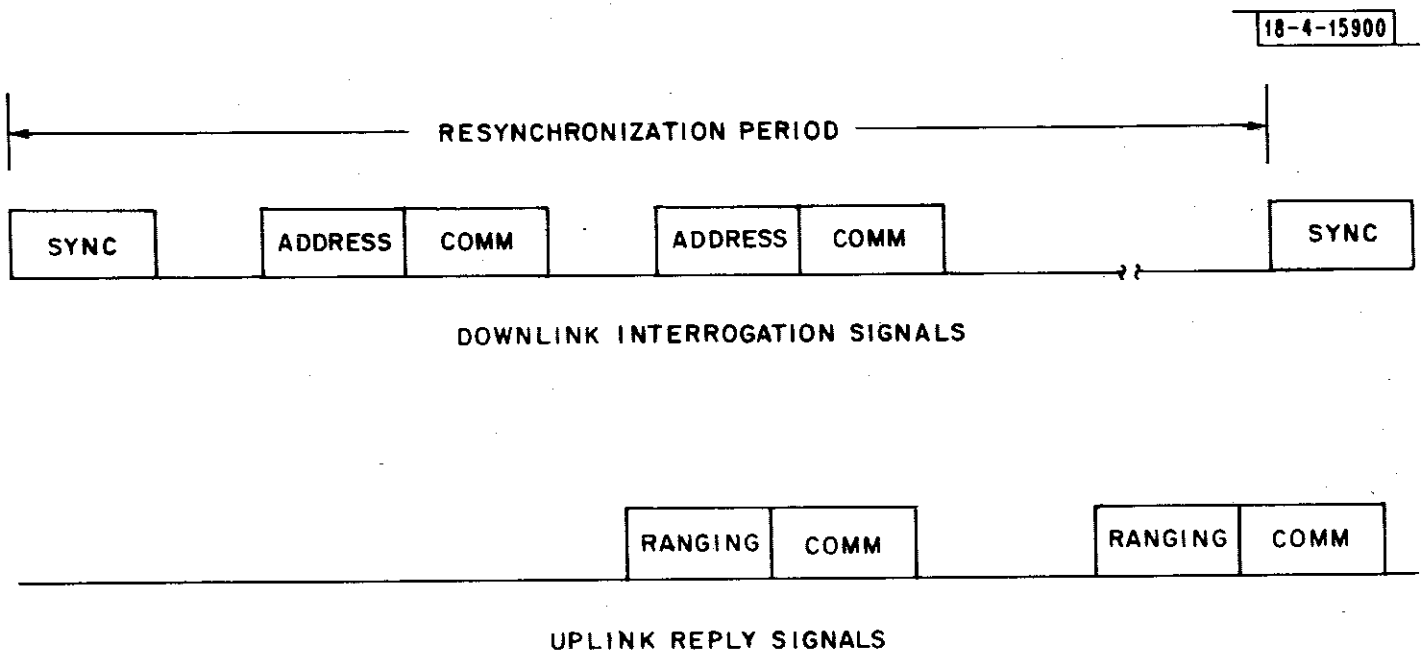

Figure 2.2. Downlink and Uplink Message Formats.

Numerous approaches to the scheduling of interrogations and replies can be devised. Elrod [12] has published a scheduling algorithm specially tailored for the ASTRO-DABS concept. For this algorithm, the airspace covered by a satellite antenna beam is decomposed into hexagonal cylinders (of maximum linear dimension 14 mi) whose axes are normal to the ground; aircraft within a cylinder are interrogated in increasing range order from the interrogator; adjacent cylinders are likewise interrogated until the airspace is exhausted. Delays are inserted between successive interrogations so that no aircraft replies overlap at the receiver satellites.

We have addressed the scheduling algorithm problem from a fundamental point of view in order to accommodate a variety of assumptions concerning signal formats and the satellite design and constellations. A summary of relevant aspects of this investigation is given in Appendix E. This includes an algorithm specialized to the representative CAST parameters of Section 1.4. In this algorithm, the airspace within a beam is partitioned into long thin rectangular solids whose axes run parallel to the ground. Actual aircraft positions are projected into virtual positions along the center line axis of each solid and aircraft are interrogated in increasing range order of virtual position from the interrogator. Parallel solids are interrogated successively until all aircraft in the beam have been interrogated. Delays are inserted between successive interrogations and between interrogation of separate regions in a manner which guarantees that there are no reply overlaps at the receivers.

For the CAST example, it is assumed that there is a single multi-beam interrogator satellite. Five of its ten beams can be used simultaneously without appreciable overlap. In a ten second period 56,000 aircraft can be interrogated* with an interrogation efficiency** of 20%.

*This is demonstrated in Appendix E.

**Interrogation efficiency (designated by the symbol η) equals the percentage of time that the interrogator satellite is transmitting interrogations downlink.

SECTION 3

TECHNICAL ISSUES

Satellite constellation, satellite antenna and avionics issues strongly impact the features of CAST. These issues are explored in this section.

3.1 SATELLITE CONSTELLATION

A variety of satellite constellations have been investigated in some detail and are reported in [13]. We shall briefly summarize the results most relevant to the considerations of this report. Various constellations ranging in size from 7 to 15 satellites were investigated. Specifically, the GDOP* has been evaluated under a variety of look angle constraints, satellite failures and CONUS aircraft locations. For aircraft in level flight, GDOP's of 6.0 can be obtained from constellations of 7 satellites, while GDOP's of 3.0 can be obtained from constellations of 15 satellites. The GDOP's for small (e.g., 7 satellite) constellations, however, increase greatly during aircraft maneuvers, or in the event of a satellite failure. By contrast, the GDOP's for large (e.g., 15 satellite) constellations are relatively insensitive to these effects. Hence, more than 7 satellites are indicated for a workable system.

One interesting constellation employs 10 satellites, of which 3 are in circular synchronous equatorial orbit and the remaining are in a synchronous

*Geometric Dilution Of Precision (GDOP) is a magnification factor which relates effective rms range error to rms position error.

elliptical orbit of eccentricity 0.35. A GDOP map for this constellation is shown in Figure 3.1. No point in CONUS has a GDOP in excess of 4.7, and the mean value is 2.4. On the average, 7 satellites are visible at any one time. This particular map is computed on the assumption that hyperbolic multilateration is used, the aircraft is not banking and the aircraft antenna exhibits usable upper hemispherical coverage at elevation angles above 15^{o}.

3.2 SATELLITE ANTENNA

Each satellite is assumed to utilize a 30 ft parabolic dish antenna. The antenna includes a feed structure which equips it for multiple beam operation. Two issues of concern are the feasibility of deploying a space qualified antenna of this sort and the number of antenna beams that this antenna requires to maintain coverage of CONUS.

The ATS-F satellite (scheduled for CY74 launch) examines the feasibility question as one of its mission objectives. It will deploy the 30 ft dish illustrated in Figure 3.2. This antenna uses an unfurlable rib structure and has a weight of under 200 pounds (including the required supporting structures) [14].

An analysis of the number of beams required for CONUS coverage and the number which are essentially disjoint is carried out in Volume II of this report. Antenna beam footprints on CONUS for a satellite at several orbital positions were computed assuming a 30 ft dish and a 1600 MHz frequency. The orbital positions were chosen from the constellation discussed in Section 3.1. The results indicate that anywhere from 3 to 17 beams might be required to maintain CONUS coverage, 10 beams being a representative number.

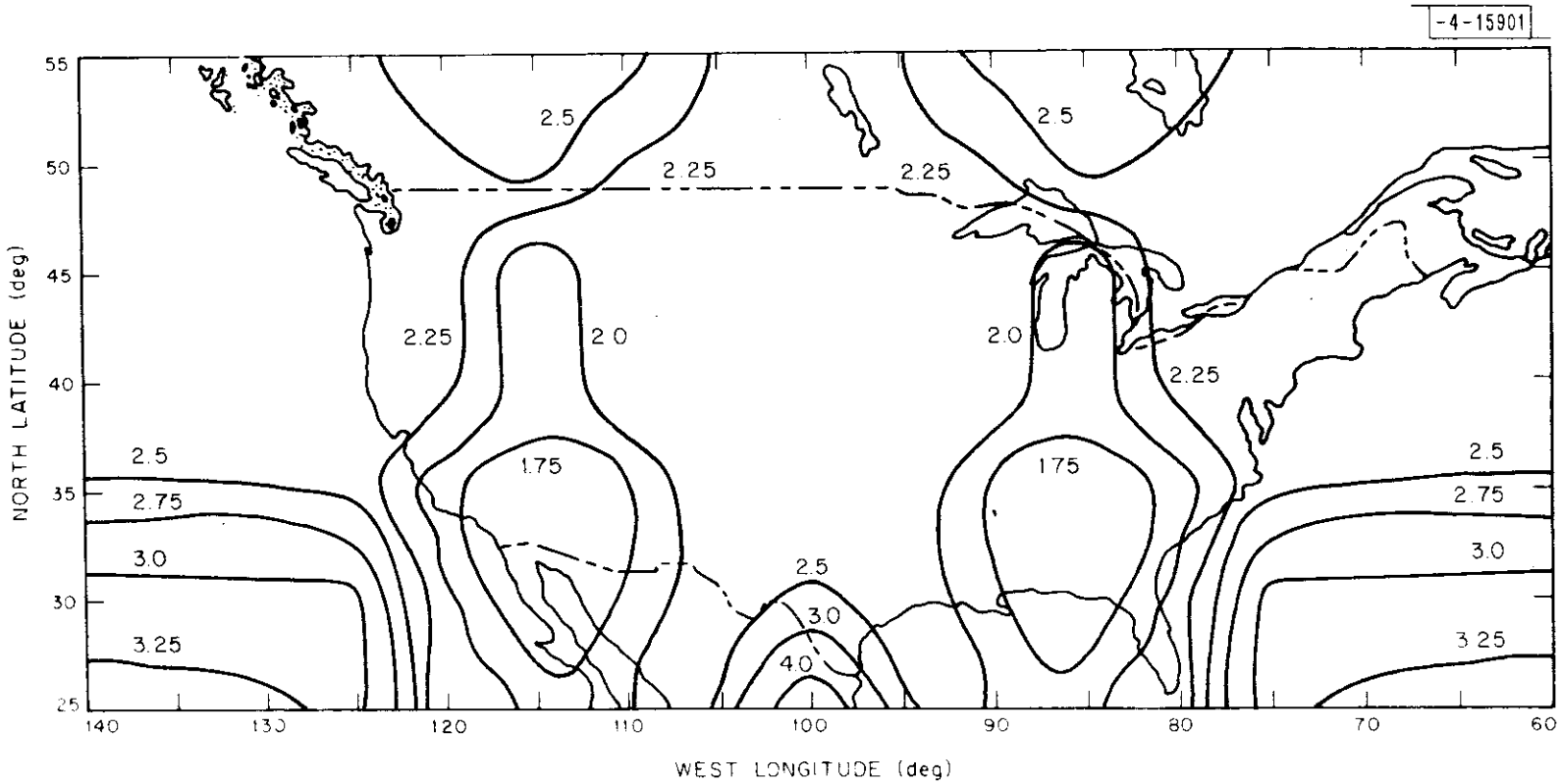

Figure 3.1. GDOP Map for a Ten Satellite Constellation.

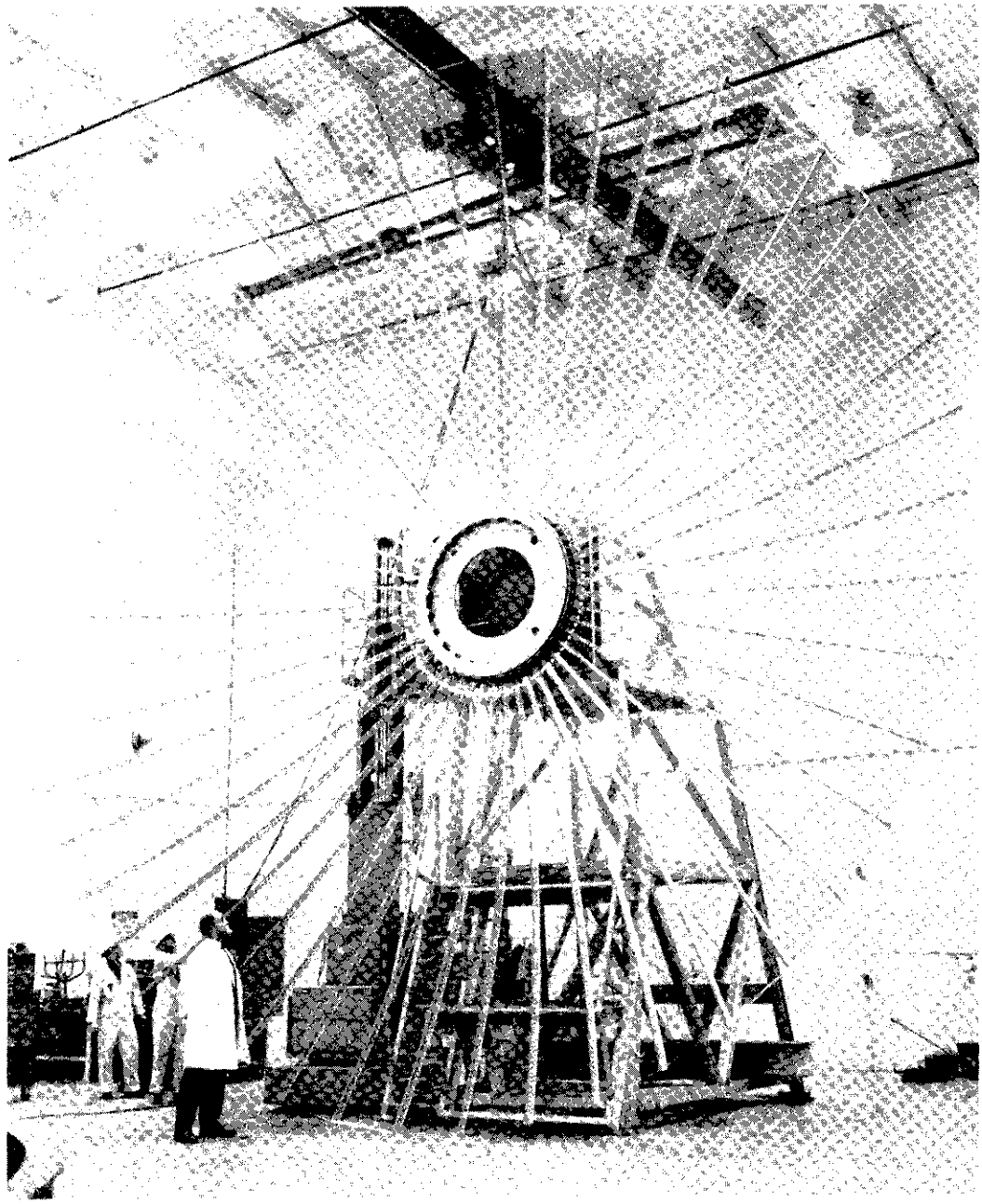

Figure 3.2. Antenna for NASA ATS-F Satellite.

Typically, 5 beams can be identified as having essentially disjoint coverage and could be selected for simultaneous use. The latter value is assumed in the sequel; however, it should be recognized that this represents an idealized assumption. A more detailed assessment should take careful account of the actual beam coverage patterns.

The premise is adopted in the ensuing analysis that the replies elicited from simultaneously interrogated aircraft will not interfere with one another at the satellite receivers; that is, it is assumed that the out-of-beam received energy is small enough to render the mutual interference negligible. This, unfortunately, will not be the case when, for example, a strong interfering reply competes with a weak intended reply. Therefore, the issue of mutual interference is not yet resolved for CAST. Techniques for abatement of mutual interference (location, separation, size of beams, etc.) have yet to be studied.

3.3 AVIONICS

Avionics considerations impact the assessment of CAST in a variety of ways. Assumptions concerning avionics affect both the performance analysis of CAST and the implied user cost burden.

To facilitate the discussion of avionics considerations for CAST, we introduce a baseline transponder; a PAM ATCRBS-like transponder. Typical receiver and transmitter characteristics of the transponder are described in the first subsection. In the next two subsections, modifications required for DPSK reception and transmission are discussed. This will enable us to study avionics in terms of both relative cost and performance.

3.3.1 General Aviation Transponders

The transponder represented by the block diagram of Figure 3.3 is similar to an ATCRBS transponder in many respects. It transmits PAM at 1030 MHz, receives PAM at 1090 MHz, and obtains synchronization by leading-trailing edge detection. The fundamental issues encountered at the frequencies assumed for CAST (1550 MHz receive/1600 MHz transmit) will differ little from those at 1030/1090 MHz.

The front end noise figure of an ATCRBS transponder is typically between 15 and 19 dB. Table 3.1 gives a nominal noise figure budget. Figure 3.4 illustrates the estimated behavior of production costs for such a receiver as a function of front end noise figure. The moderate cost increment involved in decreasing the noise figure from 15 to 11 dB reflects such relatively low cost improvements as a lower insertion loss diplexer and a lower noise figure IF amplifier first stage. The cost of the front end increases markedly if the noise figure is required to be below 10 dB, since in this region a preamplifier appears to be necessary.

Table 3.1. Receiver Noise Figure Budget for an ATCRBS-Type Transponder.

CABLE LOSS.	1 dB
DIPLEXER-PRESELECTOR FILTER INSERTION LOSS	4 dB
MIXER CONVERSION LOSS	5 dB
IF AMPLIFIER NOISE FIGURE.	5 dB
NOISE FIGURE	15 dB

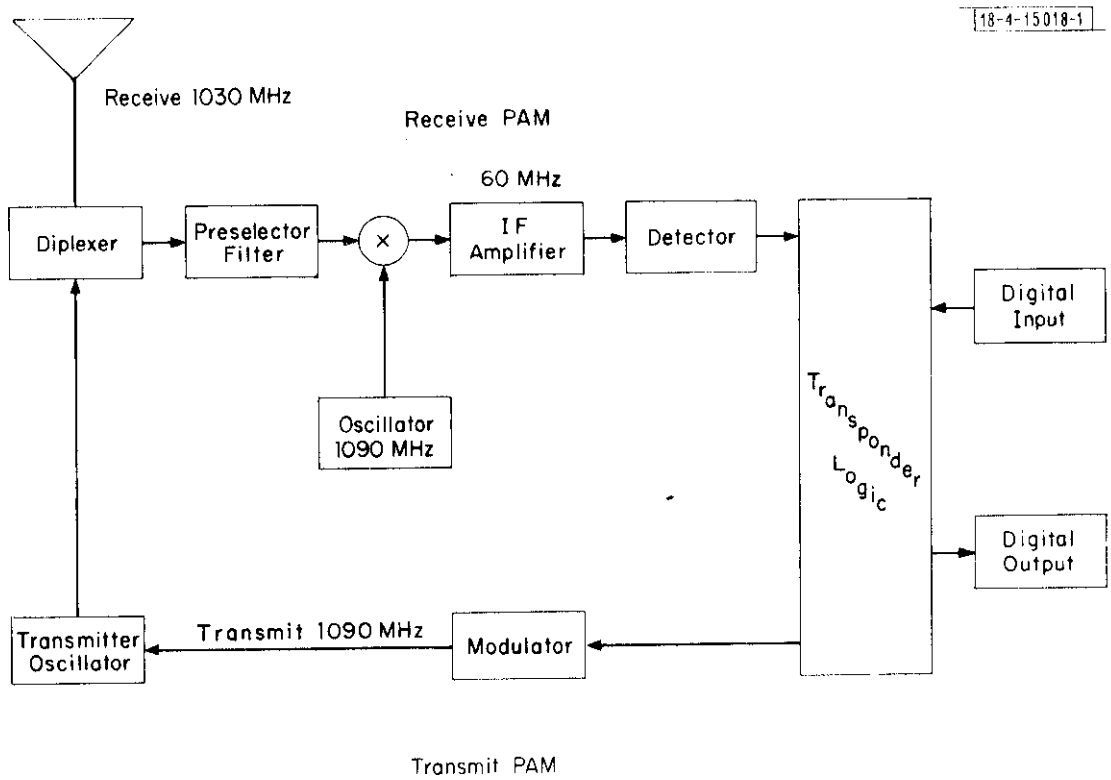

Figure 3.3. Block Diagram of an ATCRBS-Type Transponder.

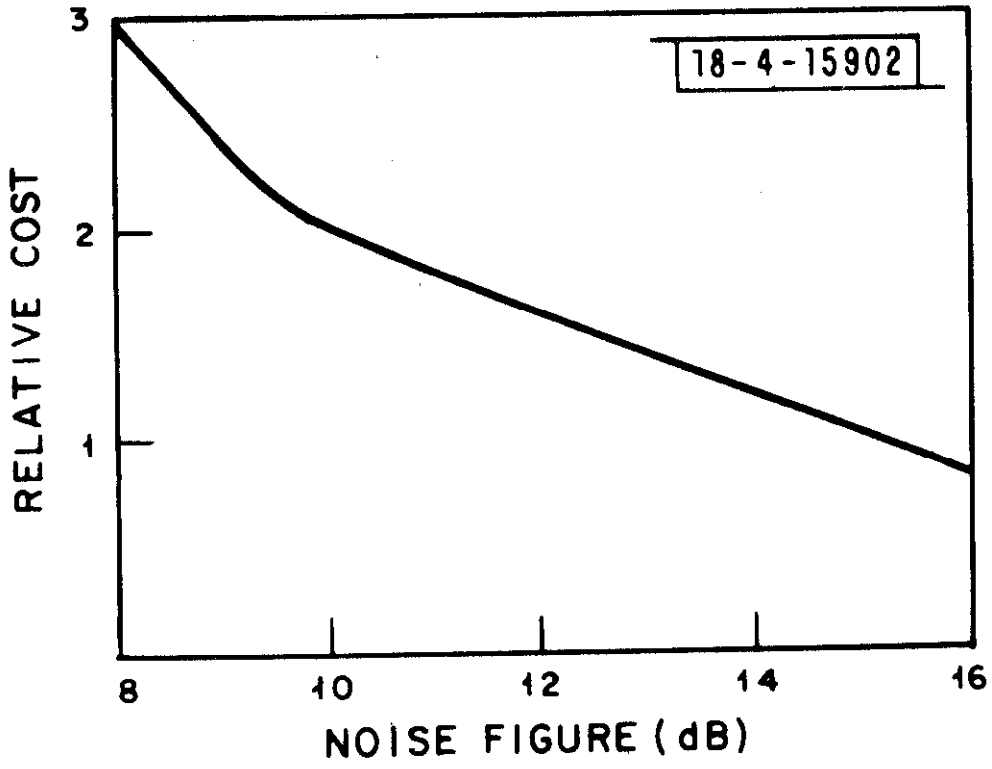

Figure 3.4. Relative Cost of Transponder Receiver vs Front End Noise Figure.

The transmitter portion typically employs a one stage pulsed triode oscillator to generate the incoherent pulsed signals. Figure 3.5 illustrates estimated behavior of production cost for an incoherent transmitter (including modulator and power supply) as a function of peak output power. For peak output powers below 500 W, the cavity can be fabricated from bent metal. When more than about 500 W peak output power is desired, a higher power tube is required and the cavity can no longer be fabricated, but instead must be machined. This occurs for a variety of reasons. The cavity is used to mechanically support the transmitter output stage tube. High output powers require larger tubes which in turn require improved mechanical support. In addition, the higher peak output power results in greater heat generation. Thermal conductivity of fabricated cavities is noticeably inferior to that of machined cavities. Machined cavities with their lower electrical loss also permit a higher overall transmitter efficiency. The RF coupling from the cavity oscillator to the antenna also has to be more carefully designed at the higher output power levels.

Figure 3.6 illustrates the functional decomposition of a receiver used in the ATCRBS-type transponder. The receiver is initially in a synchronization mode. For synchronization, the output of the matched filter must exceed a threshold in order to establish detection of the synchronization signal. When the threshold is exceeded, the peak detector is used to ascertain time of arrival. This measured time of arrival triggers the master clock which is used by all subsequent processing as a timing reference. The IF stage output is now switched into a parallel circuit for demodulation of the address and communication message.

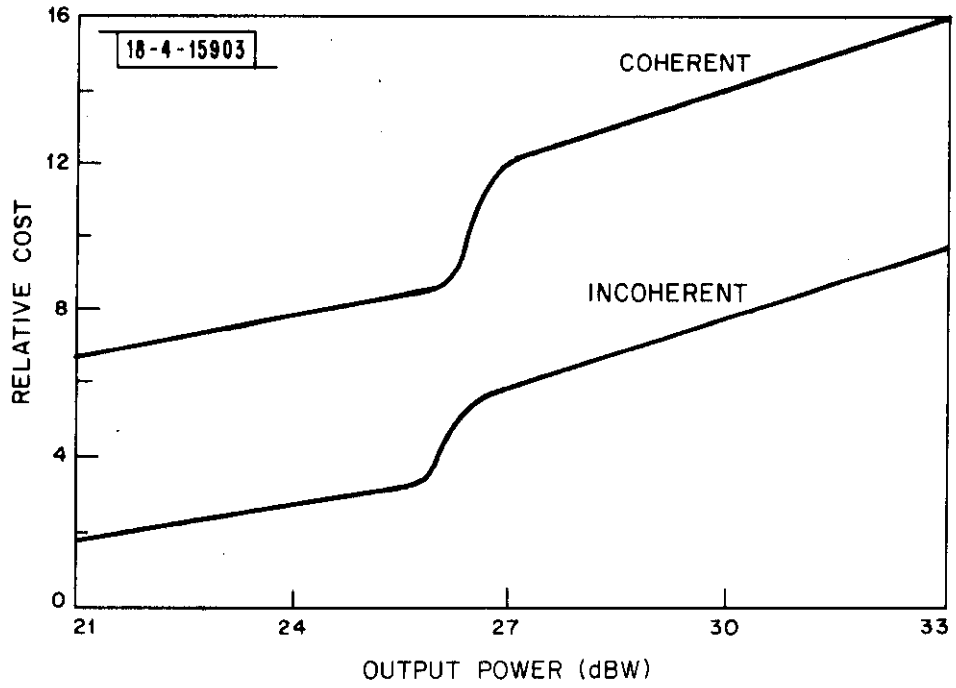

Figure 3.5. Relative Cost of Coherent and Incoherent Transmitters.

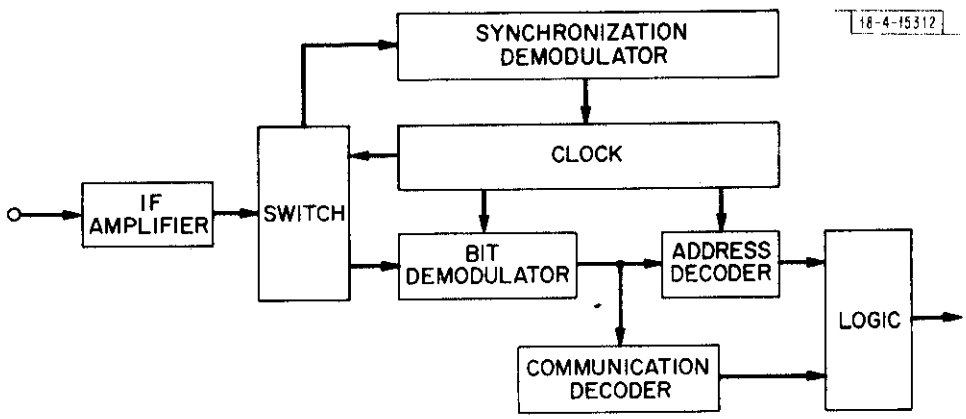

Figure 3.6. Block Diagram of Transponder Receiver.

After a prespecified delay, the address bits are demodulated and are compared (by a logical "exclusive or" circuit) to the corresponding bits in the aircraft address. The number of disagreements is counted and if that number exceeds a threshold, the address word is rejected. If, at the end of the address word, the threshold has not been exceeded, then the codeword is decoded as the aircraft address.

At a second fixed delay, decoding of the communication begins. (If the chip rate of the communication signal differs from that of the address word, the logic must be clocked at a different rate. As long as all the chip durations are multiples of the clock period, the logic need only be designed to work at the highest chip rate.) The decoded data by-passes the comparator and threshold used for address decoding and is fed to logic circuitry which formats and routes the message to the appropriate readout device.

3.3.2 DPSK Receiver

Let us now examine the details of the receiver processing when binary PSK modulation is used on the downlink. The PSK synchronization processing can be accomplished in a number of ways. For example, the synchronization demodulator might merely consist of a filter matched to the synchronization signal. Synchronization is achieved by detecting the peak of the filter output envelope. A realization of the filter by means of a Surface Acoustic Wave (SAW) device is anticipated to offer attractive cost and performance benefits.

An elementary DPSK modulator is shown in Figure 3.7. The IF signal is mixed down to a lower second IF at which the chip matched filtering takes place. The matched filter output is delayed by the chip length and

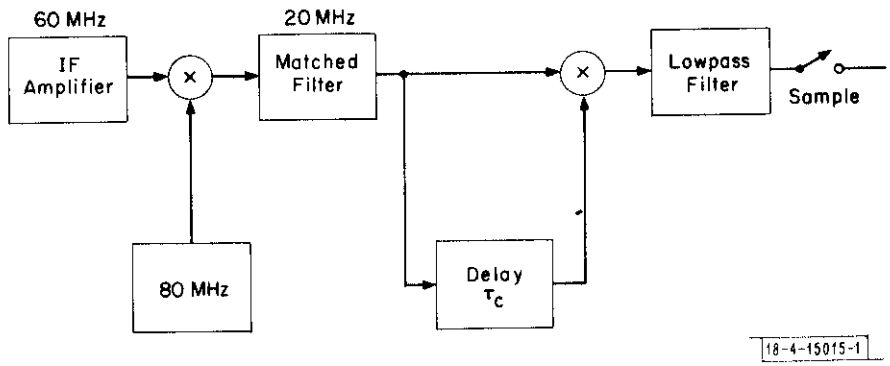

Figure 3.7. DPSK Chip Demodulator Using Two IF Frequencies.

multiplied by the undelayed version. The IF second harmonic component of the product is eliminated by the lowpass filter, and decisions are made by a polarity test on an appropriately timed sample of the lowpass component of the product.

The performance of the demodulator is sensitive to phase errors in the delay line (a 30^{o} phase error is equivalent to a 3 dB loss in signal-to-noise ratio). These errors can result from temperature variations in the aircraft. Inexpensive IF delay lines have temperature coefficients large enough to require temperature regulation.

In summary, it appears that the cost of the IF components of a DPSK receiver will not be large relative to the cost of the RF front end, especially if low noise figures are desired. The matched filter receiver is, however, more expensive than the leading-trailing edge detector counterpart in a PAM ATCRBS transponder.

3.3.3 DPSK Transmitter

By replacing the PAM transmitter of Figure 3.3 with a DPSK transmitter, the representative transponder can be made to operate in a "transmit DPSK" mode. There are principally two ways in which to implement a transmitter for incorporation into the transponder. These implementations are termed "Low Level DPSK" and "High Level DPSK."

A block diagram of a Low Level DPSK transmitter is illustrated in Figure 3.8. It uses a crystal oscillator which produces a coherent low level signal at a fundamental of the order of 100 MHz. For purposes of illustration, the frequency of the crystal oscillator output is shown to be 200 MHz, and its peak power is at 10 mW.

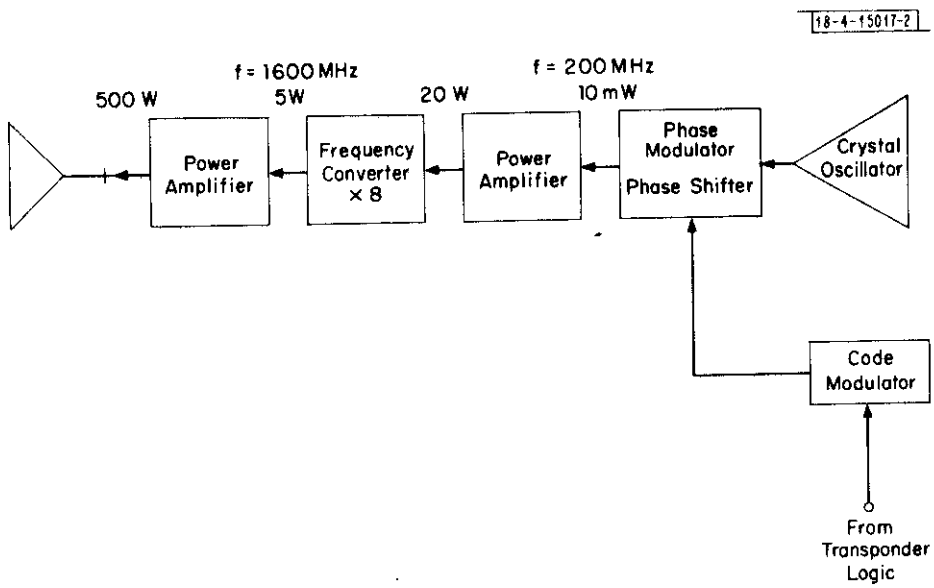

Figure 3.8. Low Level DPSK Transmitter.

The low level output of the crystal oscillator is supplied to a phase modulator which is driven so as to produce the required uplink ranging and communication signals.

The uplink signals which are produced must be brought up to the desired peak power and frequency. They are first supplied to a power amplifier which might bring the low level peak signal power up to the range of 20 W. The resultant signal then has its frequency up-converted to the transmit frequency (in this case, 1600 MHz). This occurs with some loss in power. The power is finally brought up to the desired level (e.g., 200 W) with an output stage power amplifier.

There are other configurations of this implementation which use more power amplifiers and frequency converters.

The High Level DPSK transmitter is illustrated in Figure 3.9. It uses a high level RF source generating a 500 W signal at the transmit frequency, e.g., 1600 MHz. The signal is supplied to a direct transmission path and a path which includes a 180 degree phase shifter. A DPSK chip is produced by closing both the source switch and the appropriate phase shift network switch for the chip duration. The switches are driven to produce the desired aircraft signature at the phase shifter output. The resultant signal is filtered in order to tailor the spectrum and is then supplied to the antenna.

The Low Level and High Level DPSK transmitters are expected to be roughly equivalent in cost today. Both are more expensive than the baseline PAM transmitter. The added cost in the Low Level DPSK implementation is due principally to the two required power amplifiers and the frequency converter. The power amplifier following the crystal oscillator could possibly

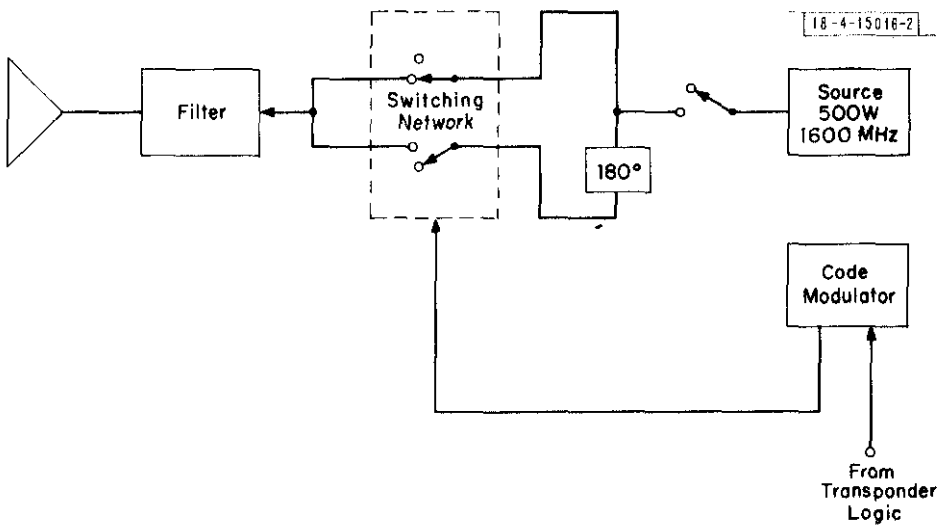

Figure 3.9. High Level DPSK Transmitter.

be built with transistors and be a low cost component. The output stage power amplifier would most likely use a high power tube, the cost of which is largely market dependent. The added cost of the High Level DPSK implementation is due principally to the switch. The switching network usually requires two PIN diodes which can be switched at the chip rate. The high level source signal generates considerable heat and thus the PIN diodes must be physically large enough to allow the heat to be dissipated without changing diode characteristics. The requirement for adequate thermal dissipation is the principal factor in the cost of the switch. It leads to an implementation cost which is comparable to that of the Low Level DPSK implementation.

The estimated production cost differential between a coherent DPSK transmitter (either High Level or Low Level) and an incoherent PAM transmitter is illustrated in Figure 3.5 as a function of the peak output power. A factor of 2-4 cost differential is evident.

SECTION 4

PERFORMANCE ANALYSIS PREREQUISITES

In this section, material is introduced which is prerequisite to a detailed analysis of systems employing CAST. First, a performance measure is developed by which different system realizations can be compared. This is followed by a presentation and discussion of the power budgets for the downlink and uplink. These provide the signal-to-noise ratios which are used to evaluate the performance measure for the various system realizations.

4.1 SYSTEM PERFORMANCE MEASURE

A central concept of CAST is that participating users share both the downlink and uplink channels. This sharing is principally in time, but is also in angle of transmission and arrival at the satellite antennas. The service provided to each aircraft requires an allotment of both downlink channel time for interrogation and uplink channel time for reply. Correspondingly, the rate at which aircraft can be serviced (users/sec) is limited by these time allotments.

For a fixed surveillance update period and number of simultaneous beam channels, this limitation upon the rate of service translates into a corresponding limit on the total number of users which can be accommodated by the system. Consequently, it is reasonable to measure system performance by the rate of service per beam.

The rate of service would not constitute a meaningful basis for comparing two system candidates if, in fact, the nature or quality of the services rendered by the two differed considerably. The precise definition of a performance measure must include some stipulation of the service goals to be achieved. Meaningful comparisons can then be made among different system realizations.

Our process of defining the performance measure is compound. First, it is recognized that CAST employs tandem operation of the downlink and uplink. Service rates for each of these can be defined separately. These rates are designated as the downlink capacity (N_d) and uplink capacity (N_u). They are defined precisely in Section 4.2 and 4.3, with respect to the reliability of service. The system performance measure, the system capacity (N), will be defined in terms of N_d and N_u as

$$N = \min(N_d, N_u) \quad . \tag{4-1}$$

4.2 DOWNLINK PERFORMANCE MEASURE - N_d

The satellite-to-aircraft link serves two essential system functions; interrogation and communication. The downlink capacity, N_d, describes the number of users that the link can service and still maintain the desired reliability of these functions. Criteria specifying the desired reliability will precede the formal definition of N_d.

Interrogation reliability actually consists of two requirements. First, when a given aircraft discrete address is transmitted by the interrogator

it must be decoded correctly at the corresponding aircraft. If this does not occur, then no reply is elicited and no updated position estimate will be made for this aircraft. Second, a given aircraft discrete address must not be erroneously decoded by some aircraft as its own address. If this occurs, a "false" reply will be transmitted and the resulting signal may generate a false target position or may interfere with the proper reception of another signal at one or more satellites. The following two parameters, P_M and P_F, measure the reliability with which interrogation is carried out.

Miss Probability:

$$P_M = \text{Prob} \left\{ \begin{array}{l} \text{on a single interrogation, the discrete} \\ \text{address transmitted to an aircraft is} \\ \text{decoded erroneously by that aircraft} \end{array} \right\} . \quad (4\text{-}2)$$

False Alarm Probability:

$$P_F = \text{Prob} \left\{ \begin{array}{l} \text{in the course of one roll call period,} \\ \text{an aircraft at least once erroneously} \\ \text{decodes an address as its own} \end{array} \right\} . \quad (4\text{-}3)$$

High reliability in communication of the downlink data is extremely important. This data may, for example, represent an IPC command from the ground, the erroneous decoding of which could result in catastrophic consequences. The following parameter, P_{bit}, is used to measure the reliability with which downlink communication is carried out.

Bit Error Probability:

$$P_{bit} = \text{Prob} \left\{ \begin{array}{l} \text{a downlink channel symbol} \\ \text{is decoded in error} \end{array} \right\} . \qquad (4\text{-}4)$$

Only binary signaling will be considered for the downlink; thus P_{bit} is the actual error probability per information bit for uncoded transmissions.

The downlink capacity can be defined in terms of constraints on P_M, P_F, and P_{bit}, constraints which represent desired downlink performance goals for CAST. It is assumed that P_M, P_F, and P_{bit} satisfy the following inequalities:

$$\begin{aligned} P_M &< 10^{-5} , \\ P_F &< 10^{-6} , \\ P_{bit} &< 10^{-6} . \end{aligned} \qquad (4\text{-}5)$$

These constraint values are reasonable representative requirements. Order of magnitude changes in their values will not be reflected in drastic changes in either the design of the system or its ultimate performance.

The constraint on P_M implies that on the average fewer than one out of every 10^5 interrogations will fail to elicit a response from the intended aircraft. For example, if interrogations are performed at the rate of 10^5 in 10 sec, then on the average, only one interrogation will fail to elicit a response over a 10 sec interval.* The constraint on P_F insures that false replies will

*Other contributions to the miss probability, e.g., aircraft antenna pattern nulls, are neglected in computing P_M.

occur with a frequency less than 10% of that of missed responses. On the average, fewer than one out of every 10^6 interrogations will elicit an erroneous response from an unintended aircraft.

In terms of the performance goals stipulated by (4-5), the downlink capacity, N_d, is now defined as

$$N_d = \left\{ \begin{array}{l} \text{the number of aircraft serviced per satellite} \\ \text{antenna beam per second, on the downlink,} \\ \text{subject to constraints of (4-5)} \end{array} \right\}. \qquad (4\text{-}6)$$

4.3 UPLINK PERFORMANCE MEASURE - N_u

The aircraft-to-satellite link serves two essential functions for each aircraft. It provides for the transmission of a ranging signal from which the surveillance information is ultimately derived and it also enables the communication of uplink data from the aircraft to the satellite. For our purposes, the uplink address transmission is considered part of the communication message. The uplink capacity, N_u, describes the number of users that the link can service and still maintain the desired reliability of these functions. Criteria establishing the desired reliability will precede the formal definition of N_u.

The times at which the ranging signal arrives at the receiver satellites are used to compute the position of the aircraft. These arrival times must be accurately measured if the surveillance function is to be executed reliably. The following parameter, $\sqrt{\overline{\epsilon_t^2}}$, measures the reliability with which the uplink ranging is carried out.

RMS Ranging Error:

$$\sqrt{\epsilon_t^2} = \left\{ \begin{array}{l} \text{the rms error, due to the receiver noise,} \\ \text{in estimating the arrival time of the} \\ \text{ranging signal at a satellite} \end{array} \right\} . \qquad (4\text{-}7)$$

The aircraft-to-satellite communications serves to complete the two-way digital data link. Again, P_{bit} can be used to measure the reliability with which uplink communication is carried out. P_{bit} in this context will be defined as

$$P_{bit} = \text{Prob} \left\{ \begin{array}{l} \text{an uplink channel symbol is} \\ \text{decoded in error} \end{array} \right\} . \qquad (4\text{-}8)$$

The uplink capacity can now be defined in terms of constraints on $\sqrt{\epsilon_t^2}$ and P_{bit}, constraints which represent desired uplink performance goals for CAST. It is assumed that $\sqrt{\epsilon_t^2}$ and P_{bit} satisfy the following inequalities:

$$\begin{aligned} &\sqrt{\epsilon_t^2} < 10 \text{ nsec}, \\ &P_{bit} < 10^{-6} . \end{aligned} \qquad (4\text{-}9)$$

These constraints are again intended to be representative goals. The constraint on $\sqrt{\epsilon_t^2}$ is designed to ensure that the undiluted rms error due to receiver noise alone in estimating an aircraft-to-satellite range does not exceed 10 ft. This constraint value was chosen for a variety of reasons. Little improvement in the total rms position error would result from reducing

the constraint on the error due to receiver noise to a value below 10 nsec, since other effects such as ionospheric delay variations and satellite position uncertainty would then dominate the overall error. On the other hand, permitting the constraint to be larger than 20 nsec would tend to make the receiver noise error the dominant contributor to the overall range measurement error. When GDOP is taken into account this could result in unacceptably large position error. Little increase in system capacity is achieved if the constraint is increased from 10 to 20 nsec.

The P_{bit} constraint actually provides for an uplink channel which is more reliable than the downlink, since, although their per bit error rates are identical, the uplink has the additional advantage of diversity through the multiple (at least four) satellite channels.

In terms of the performance goals stipulated by (4-9), the uplink capacity, N_u, is now defined as

$$N_u = \left\{ \begin{array}{l} \text{the number of aircraft service per satellite} \\ \text{antenna beam per second, on the uplink, subject} \\ \text{to the constraints of (4-9)} \end{array} \right\} . \quad (4\text{-}10)$$

4.4 DOWNLINK POWER BUDGET

The received signal-to-noise ratio in the satellite-to-aircraft downlink is computed in the power budget given in Table 4.1. The computation is made under the assumption that the downlink carrier frequency is 1550 MHz, an allocation in the Aeronautical Radionavigation Band. Each entry in the budget is now discussed.

Table 4.1. Representative Downlink Power Budget.

Transmitted Peak Power	30 dBW	1 kW
Peak Satellite Antenna Gain	42 dB	30 ft dish
Thermal Distortion	-2 dB	
Antenna Shadowing	-1 dB	
Off Boresight Loss	-3 dB	Aircraft at beam edge
Maximum Path Loss	-192 dB	Synchronous elliptical orbit, 1550 MHz
Atmospheric Effects	-1 dB	
Minimum A/C Antenna Gain	-1 dB	Elevation above 15°
Received Peak Power	-128 dBW	
Received Noise Power Density	-193 dBW/Hz	3600°K, 11 dB noise figure
Received Peak Power to Noise Power Density	65 dB/sec	

The entry corresponding to "transmitted peak power" is well within the capability of current technology. At present, space qualified helix TWT's exist which can generate pulsed signals at L-band having; 1 kW peak power, durations of up to 100 μsec and 25% duty cycle. Improved space qualified TWT's which can generate pulsed L-band signals having 2-3 kW peak power, durations of 100's of μsec and 50% duty cycle may be possible.

The entry for "peak satellite antenna gain" corresponds to 1550 MHz operation of the 30 ft multibeam satellite antenna discussed in Section 3.2.

The thermal distortion and antenna shadowing entries account for non-ideal satellite antenna characteristics. The thermal loss represents distortion of the dish shape due to solar heating. This entry is based upon an estimate made for the ATS-F antenna [14]. The shadowing loss reflects the pattern distortion due to the feed structures.

In order to insure that the quality of service with CAST meets the requirements specified in Section 4.1 for almost all users, the received power level is referred to a disadvantaged user in the system. This user is taken to be an aircraft which is located at a point on the 3 dB footprint contour of one of the beam patterns. A 3 dB "off boresight loss" in the budget accounts for this.

The "maximum path loss" entry is calculated for a 35,000 mi path at 1550 MHz. This corresponds to the distance to a satellite at the apogee of an elliptical (eccentricity 0.35) synchronous orbit, one of the orbits included in the illustrative satellite constellation introduced in Section 3.1.

Atmospheric effects such as absorption, dispersion and refractive increase of path length are accounted for by a 1 dB loss.

The choice of aircraft antenna must be consistent with the required inclusion of general aviation aircraft users in the CAST system. High gain antennas requiring complex steering subsystems are inconsistent with the cost constraints of the general aviation aircraft market. Instead, it will be assumed that aircraft being serviced by the CAST system use a top mounted antenna with essentially uniform upper hemispherical coverage (an example is a crossed slot antenna). This allows for the coverage of a widely dispersed (in both azimuth and elevation) satellite constellation. The entry for aircraft antenna gain is taken from [15, Appendix A.5] and is representative of the minimum gain of the measured pattern at elevation angles above 15^{o} relative to the plane of the aircraft (an aircraft banking 30^{o} away from a satellite at 45^{o} elevation could encounter the minimum gain).

The choice of an 11 dB noise figure requires a front end which is improved relative to that of present day general aviation ATCRBS transponder. However, as noted in Section 3.3, the added costs are moderate and thus this value represents a good first order engineering choice. At this noise figure, receiver noise completely dominates other noise sources such as galactic noise and RFI.

The resulting received peak power to noise power density is 65 dB/sec, which means that, for example, a pulse of 1 μsec duration would be received with a 5 dB signal-to-noise ratio.

4.5 UPLINK POWER BUDGET

The received signal-to-noise ratio in the aircraft-to-satellite uplink is computed in the power budget given in Table 4.2. The assumed uplink frequency is 1600 MHz which, like the downlink frequency, is within the Aeronautical Radionavigation Band. Many of the entries in the power budget are identical to corresponding entries in Table 4.1, the downlink power budget.

Following the discussion in Section 3.3, the transmitted peak power of 500 W represents a sensible engineering choice, i.e., it is at the breakpoint of the transmitter cost curve, Figure 3.5. Transmitter costs increase markedly as peak transmitter power increases above 500 W.

The transmitter power disadvantage accounts for cable losses between transmitter and antenna, aging, and nonuniform quality in manufacture. The 3 dB loss is an estimate. Colby and Crocker [16] have made measurements of the output power in transponders already installed in aircraft. Their measurements show much greater variations than the indicated 3 dB loss; hence, this estimate is optimistic for today but perhaps realistic for 10 to 20 years hence.

The decorrelation loss term accounts for the mismatch between the transmitted signature and the matched filter receiver. Mismatch could result from Doppler shift due to aircraft motion relative to the satellites, fixed carrier frequency offset in the aircraft transmitter and/or a frequency chirp in the transmitted signature. The loss in effective signal energy for a matched filter envelope detector with a frequency offset of Δf and integration time τ is given by $(\sin \pi \Delta f \tau / \pi \Delta f \tau)^2$. A 1 dB loss corresponds to an offset-

Table 4.2. Representative Uplink Power Budget.

Transmitter Peak Power (at antenna)	27 dB	500 W
Transmitter Power Disadvantage	-3 dB	
Decorrelation Loss	-1 dB	Oscillator drift, relative motion
Minimum A/C Antenna Gain	-1 dB	Elevations above 15°
Path Loss	-192 dB	Synchronous elliptical orbit, 1600 MHz
Atmospheric Absorption	-1 dB	
Peak Satellite Antenna Gain	42 dB	30 ft antenna at 1600 MHz
Off Boresight Loss	-3 dB	
Thermal Distortion	-2 dB	
Antenna Shadowing	-1 dB	
Received Peak Power	-135 dB	
Noise Power Density	-201 dBW/Hz	600° K, thermal, galactic noise and RFI
Received Peak Power-to-Noise Ratio	66 dB/sec	

duration product of $\Delta f\tau \simeq 0.3$. As an example, for a 20 μsec integration time the corresponding frequency offset is 15 KHz (equivalently, one part in 10^5). This represents a modest requirement even for inexpensive avionics [17].

The receiver noise is composed of thermal, galactic and RFI contributions. No comprehensive program of measurement of these noises at L-band has been carried out. Here a receiver noise temperature at the satellite of 600° K is assumed. This is not an unreasonable assumption in light of available VHF data [18].

The remaining entries have been described in Section 4.4. The The resultant received peak signal power-to-noise power density ratio is 66 dB/sec, which means that, for example, a pulse of duration 1 μsec would be received with a 6 dB signal-to-noise ratio.

SECTION 5

DOWNLINK PERFORMANCE ANALYSIS

In this section, the performance of the satellite-to-aircraft downlink will be examined by computing the downlink capacity N_d. We will show that with CAST the downlink can reliably service as many as 30,000 aircraft with a 10 second update period, provided that the downlink signaling is executed using DPSK and the aircraft transponder has a front end noise figure of, at most, 11 dB. This service figure assumes that the efficiency of the interrogation algorithm is 10%, 5 of the 10 satellite antenna beams are used simultaneously and the downlink and uplink communication messages are each composed of 20 bits.

N_d, the downlink capacity, is a function of the method by which the downlink signaling is carried out. Specifically, it depends upon: the type of modulation employed, the method of encoding the discrete addresses, the method of encoding the communication messages, and the method by which synchronization is established and maintained. The many different choices for each of these methods lead to many alternative ways of executing the downlink signaling. The choices considered in examining downlink performance will be presented and discussed before the link capacity is computed and conclusions are drawn.

5.1 MODULATION

Two modulation candidates are considered; binary PAM and binary DPSK. Both performance and avionics issues motivate these choices. These issues are discussed in turn.

The relative performance of these two candidates is demonstrated quite clearly by the bit error probability parameter, P_{bit}, defined in (4-4). Figure 5.1 illustrates the variation of P_{bit} with E_c/N_o, the signal energy-to-noise power density ratio of a received chip. The curves describe the performance of the optimum receivers for the random phase channel with perfect synchronization.*

As is evident and well known, DPSK is 6 dB more efficient than PAM, i.e., for a given transmitter power DPSK can utilize shorter duration waveforms for communications and address. Thus, it can achieve a higher value of N_d.

The choice of modulation cannot be based upon performance alone. Cost considerations are equally important. As we have pointed out in Section 3.3, binary PAM receivers are used in present day ATCRBS transponders. DPSK matched filter receivers are not in such use and are more expensive; low cost approximations to DPSK matched filter are possible with, however, reduced performance.

---

*The random phase channel is characterized by received signals of known waveform and total energy, but uniformly distributed phase angle. To the signal is added white Gaussian noise of zero mean and power density N_o W/Hz (single-sided). This is the assumed downlink channel model.

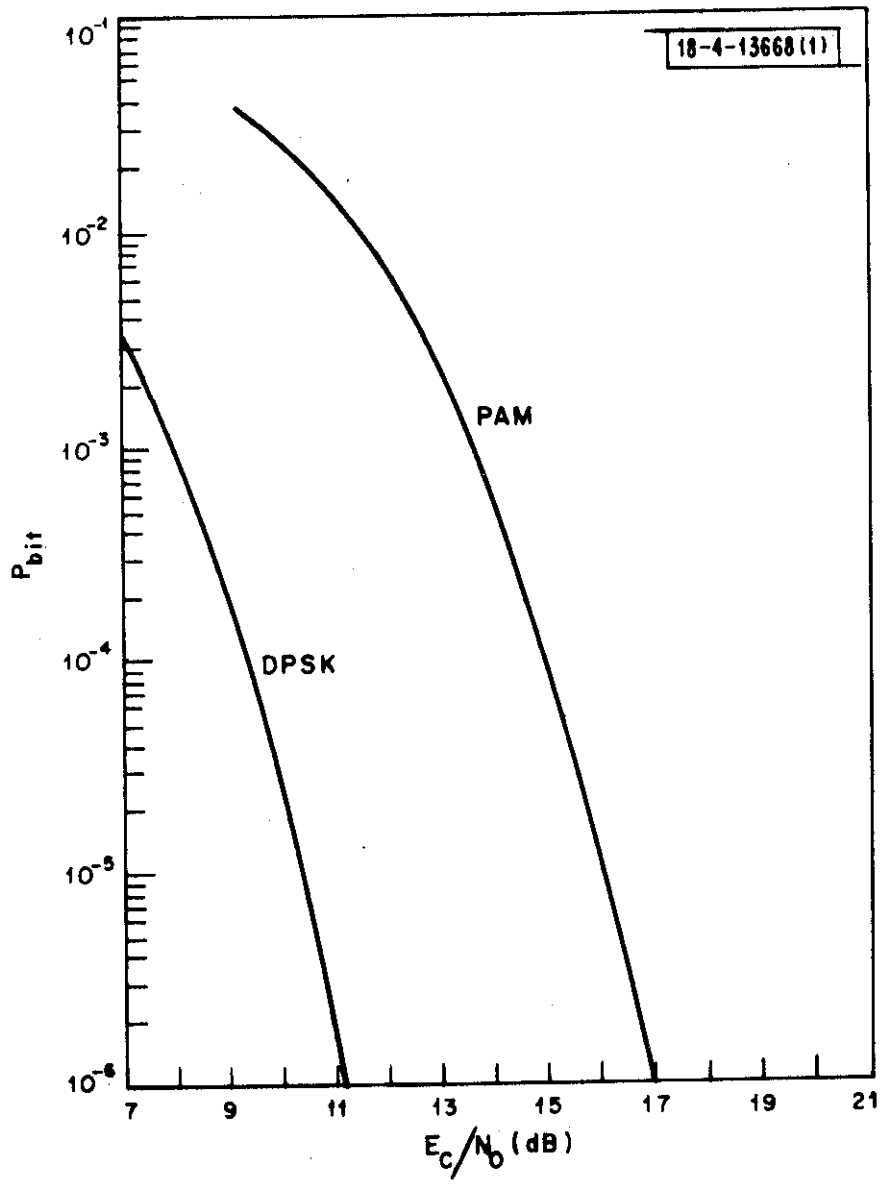

Figure 5.1. Bit Error Probabilities vs Signal-to-Noise Ratio for PAM and DPSK Modulation.

5.2 ADDRESS AND COMMUNICATION FORMAT

The signaling format assumed for the downlink address and communications was discussed in Section 2.2. It is instructive, nevertheless, at this point, to briefly digress and mention some alternative formats which might have been pursued and to compare their features with those of the assumed format.

To recapitulate, in the assumed format the aircraft address and communication message are treated as separate binary words (of length n_a and n_c bits, respectively) which are transmitted serially. One or both of these words could be encoded in some fashion to provide increased protection against channel errors. The issues of decoding complexity arising from the use of coding are discussed separately for the address and communications in Section 5.3 and 5.4.

An address overlay technique is an alternative to the above format. In this case, it is assumed that prior to transmission the communication message is encoded by a linear $(n_c + n_a, n_c)$ code.* The encoding is systematic, which means that the n_c uncoded message digits appear at the beginning of the codeword and are followed by n_a parity check digits. The aircraft address is overlaid** on the parity bits, and the resulting $(n_c + n_a)$ - digit word is transmitted.

In comparing the two formats, it is apparent that the overlay method offers greater redundancy in the communication encoding at no expense in

*An (n, k) codeword contains n binary digits, of which k are information digits. See Appendix A for a more complete discussion of linear codes.

**Added to the parity bits modulo 2.

total message length. However, decoding of the address and communications are as a result interdependent. This is not the case for the separate word format. The nature of this interdependency appears to be such that the overlay method offers good protection in an interference environment in which bursts of several adjacent digit errors may occur [19]. In a random error situation, one finds that only a few errors in the received message digits can cause many errors in the address decoding unless some error correction is implemented. With CAST, each aircraft receives a large number of interrogations which are intended for other aircraft. This could cause a potential false alarm hazard which may be intolerable. Thus, the assumed separate word format is preferred for the ensuing CAST system analysis.

5.3 ADDRESS ENCODING

Each user aircraft in CAST is supplied a unique discrete address. It will be assumed that CAST is operating in an environment which contains as many as 10^6 aircraft [20]. In order to accommodate an aircraft population of 10^6, an equal number of unique discrete addresses is required.

For illustrative purposes, we consider two of the many possible methods for encoding the discrete address for transmission in the satellite-to-aircraft link. These are designated as uncoded and coded address format and are now described.

5.3.1 Description of Address Set Candidates

In the uncoded format, each aircraft is assigned a unique 20 digit binary sequence as its address word. Each of the 2^{20} such sequences is

eligible to be an address. Since an error in any one bit transforms one address into another, the miss and false alarm probabilities of the uncoded format can be kept small only by controlling the bit error probability.

In the coded format, each address is chosen to be a sequence of n binary digits, $n > 20$. Of the 2^n possible binary sequences, 2^{20} are chosen as the address set. These address words are chosen to be as dissimilar as is possible in order to minimize P_F, the false alarm probability.

The following simple form of decoding can be employed at the transponder for either format. The number of digit disagreements between a received address and the aircraft's own address is computed. If the number does not exceed a threshold T, the address is decoded as that of the aircraft. For the uncoded format, $T = 0$. Since this decoding rule requires very little more complexity in transponder logic in the coded case than it does in the uncoded case, it is reasonable to assess the merits of the two address formats on the basis of performance.

5.3.2 Code Specification and Performance

We restrict consideration to linear (n, k) binary codes where n is the block length and k is the length of the binary sequence to be encoded. The miss and false alarm probabilities (P_M and P_F) which result from the use of such codes are derived in Appendix A. These results are summarized in Table 5.1 for a miss probability $P_M \leq 10^{-5}$. *

*In Table 5.1 E_a designates the received energy in the full address word.

Table 5.1. Performance of Uncoded and Coded Address Formats for $P_M \leq 10^{-5}$.

Address Encoding	$E_a/N_o\|_{PAM}$(dB)	$E_a/N_o\|_{DPSK}$(dB)	P_F
Uncoded Format	30.4	24.4	1.00×10^{-5}
Linear (n, k) Code			
(31, 20)	29.4	23.4	2.16×10^{-6}
(41, 20)	29.1	23.1	3.90×10^{-7}

The results displayed in the above table may be summarized as follows. For both PAM and DPSK, an increase in the block length (n) is accompanied by decreases in both the signal-to-noise requirement for the address word and the false alarm probability P_F. The former is reflected in a decrease in codeword duration. As a result, a corresponding increase in the capacity N_d can be expected. The changes in duration are more dramatic in the transition from the uncoded case to the (31, 20) code than in the transition from (31, 20) to (41, 20). This suggests that much of the benefit to be derived from the use of the coded format is acheived by the (31, 20) code. This code is used in the sequel for the computation of the downlink capacity.

5.4 COMMUNICATION MESSAGE ENCODING

The performance benefits which result from employing coded address formats on the downlink are a stimulus for considering similar formats for the communication messages. In general, full exploitation of the random

error correcting capability of a linear code may impose some computational burden but will provide improved performance. For present purposes, we shall consider only binary uncoded format. The number of bits to be communicated per interrogation is left as a parameter in the computation of N_d.

Table 5.2 can be used to compare the communication performance of the two modulation candidates. The table indicates the E_c/N_o* and bit duration required in order to obtain the desired $P_{bit} = 10^{-6}$. The downlink power budget (Table 4.1) was assumed in computing this table. The superiority of DPSK is evident.

Table 5.2. Downlink Communication Requirements.

Modulation	E_c/N_o(dB)	Chip Duration (μsec)
PAM	17.2	16.8
DPSK	11.2	4.2

*E_c is the received energy in the communication chip.

5.5 TIMING AND SYNCHRONIZATION

Synchronization is obtained on the downlink by having the satellite transmit a synchronization signal periodically to all aircraft users. This signal establishes a timing reference that can be used over the resynchronization period. A variety of signals which may serve this purpose are analyzed in this section. Several error mechanisms can degrade the accuracy of the timing reference established by the synchronization signal. Specifically, errors due to clock instability, relative motion and time of arrival estimation can decrease the downlink capacity. We will conclude this section by examining these effects.

The type of synchronization signal that can be used is dependent upon the modulation employed. In examining downlink performance, a single candidate synchronization signal is considered for each type of modulation.*

5.5.1 PAM Synchronization Signal

The PAM waveform considered for synchronization is a single, constant amplitude pulse. It is assumed that a maximum likelihood estimate of the TOA is made by passing the received pulse through a matched filter and linear envelope detector and choosing as the arrival time estimate the time at which the detector output is maximum [21]. It has been shown that the root mean squared error, $\sqrt{\epsilon_t^2}$, in making an arbitary TOA estimate for the pulse is lower bounded by [22]

*It is assumed that the synchronization signal uses the same modulation as the address and communication signals.

$$\sqrt{\overline{\epsilon_t^2}} \geq \sqrt{\frac{.1}{(P/N_o)^2}} \quad \text{sec} \tag{5-5}$$

where P/N_o is the received peak power-to-noise power density ratio.

For P/N_o = 65 dB/sec (see power budget, Section 4.4), (5-5) yields an rms error of at least 100 nsec in estimating the TOA of the synchronization signal. An increase in signal-to-noise ratio obtained by increasing the pulse length will not further decrease the TOA error.

It can be shown that $\sqrt{\overline{\epsilon_t^2}}$ is accurately approximated by the lower bound of (5-5) if E_s/N_o, the synchronization signal energy-to-noise power density ratio, exceeds a threshold value of 15 dB [23, 24]. In order to achieve a 15 dB signal-to-noise ratio, a pulse duration of 40 μsec is required.

5.5.2 DPSK Synchronization Signal

In contrast to PAM square pulse synchronization, the synchronization error is not solely a function of the received peak power-to-noise power density ratio. Decrease in synchronization error can be achieved by increases in the signal time-bandwidth product and/or the peak power. For this reason a binary phase coded signal whose autocorrelation function has low sidelobes is an attractive candidate for a DPSK synchronization signal. The signal considered here is a 31 bit maximal length sequence having a peak to maximum sidelobe ratio of approximately 10. The chip duration, τ_c, of this signal is specified at 1.25 μsec and the chip rise time, t_r, at 50 nsec.* Including a DPSK reference chip, the total waveform duration, T_s, will be 40 μsec.

*This rise time implies a bandwidth on the order of 10 MHz, which is not unreasonably large for the assumed frequency allocations.

It is again assumed that synchronization is obtained by first passing the received signal through a matched filter linear envelope detector, and then choosing as the arrival time estimate the time at which the detector output is maximum.

The required performance analysis has been carried out by Orr and Yates [22]. They have obtained a lower bound to $\sqrt{\overline{\epsilon_t^2}}$, the rms arrival time error, as a function of: the synchronization signal-to-noise ratio (E_s/N_o), the a priori uncertainty in the TOA, and the chip parameters (duration and rise time). Figure 5.2 shows a graph of $\sqrt{\overline{\epsilon_t^2}}$ as a function of E_s/N_o for the specific DPSK synchronization signal assumed. For a duration T_s = 40 μsec and a received P/N_o = 65 dB/sec (see Section 4.4), the signal-to-noise ratio is E_s/N_o = 21 dB. The corresponding rms error is less than 10 nsec.

5.5.3 Effect of Timing Errors on Downlink Performance

We will now consider the effect of the various timing errors on downlink performance. Errors due to clock instability and relative motion will be considered first. The effect of synchronization signal TOA estimation error is dealt with second.

The errors due to clock instability and relative motion of the aircraft arise in the following way. For a given aircraft, it may be the case that the interval which elapses between the establishment of synchronization and the interrogation of that aircraft is quite long. During that interval there may be a buildup of timing error due to both discrepancies between the on-board and satellite clock rates and relative motion of aircraft and satellite. The clock error may be treated as deterministic to the extent that clock accuracies

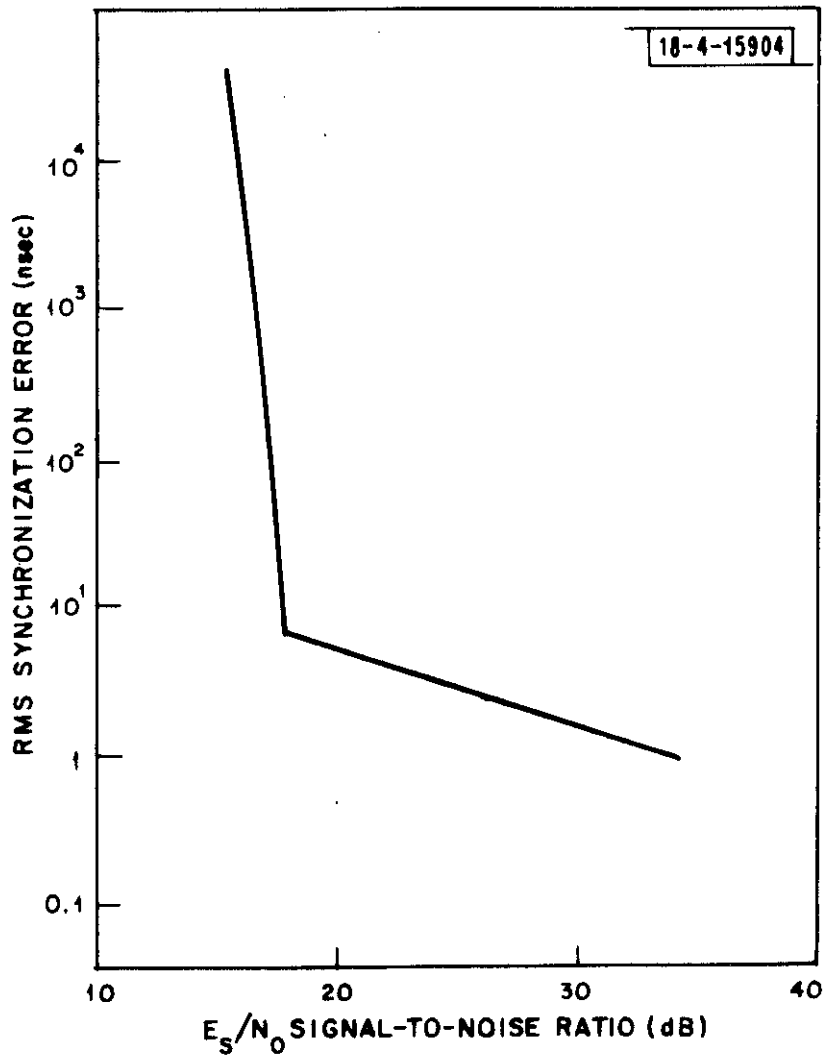

Figure 5.2. Downlink Synchronization rms Error vs Signal-to-Noise Ratio for DPSK Modulation.

are specified to a tolerance of δ_c sec/sec. Even allowing the worst case error to occur, the sampling time error is bounded by

$$|\Delta t|_{clock} < \delta_c t \tag{5-5}$$

where t is the elapsed time since synchronization. Similarly, if an aircraft and interrogator satellite move at maximum relative velocity V_{rel}, then the corresponding timing error is bounded by

$$|\Delta t|_{motion} < \left(\frac{V_{rel}}{c}\right) t \quad . \tag{5-6}$$

These two errors are of similar nature and may be combined into a single term by defining

$$\delta \triangleq \delta_c + \frac{V_{rel}}{c} \quad . \tag{5-7}$$

The worst case error t seconds from synchronization is thus δt.

The clock and relative motion errors can have a marked effect on P_{bit} and thus on downlink performance. As modeled here, they are cumulative and will eventually cause significant degradation in P_{bit}. If the resynchronization period is x sec, the synchronization error at the end of the period due to these two errors could be as much as δx sec. In demodulating the communication chips, this would translate into an effective loss in E_c/N_o. The extent of the loss is a function of the modulation. If the communication chips are sufficiently elongated, this loss will be equalized and the effective signal-to-noise

ratio in the chip will once again be E_c/N_o. This procedure is discussed more fully in Appendix C, where it is shown how the resynchronization period is chosen to maximize N_d in the presence of clock and relative motion errors.

We now quote the result of the Appendix C analysis. Let

T_s = Duration of Synchronization Signal

τ_a = Duration of Address Chip

τ_c = Duration of Communication Chip

n_a = Number of Address Chips

n_c = Number of Communication Chips

η = Interrogation Efficiency

δ = Maximum Timing Error/sec

and define

$$\text{(PAM)} \qquad T_{tot} = n_a \tau_a + n_c \tau_c \text{ sec}$$

$$n_{tot} = n_a + n_c$$

$$\text{(DPSK)} \qquad T_{tot} = (n_a + 1)\tau_a + (n_c + 1)\tau_c \text{ sec}$$

$$n_{tot} = n_a + n_c + 2 \quad .$$

The resynchronization period which will maximize N_d, given δ, is

$$\tilde{x} = T_s \left[1 + \sqrt{\frac{T_{tot}}{4\, n_{tot}\, \delta\, T_s}} \right] \text{ sec} \quad , \tag{5-8}$$

and the corresponding optimum value of N_d is

$$N_d(\tilde{x}) = \frac{\eta / T_{tot}}{\left[1 + \sqrt{\frac{4\, n_{tot}\, \delta\, T_s}{T_{tot}}} \right]^2} \text{ aircraft} \quad . \tag{5-9}$$

The capacity evaluations in Section 5.5 are based upon (5-9).

We now consider the effect of synchronization signal TOA estimation error by demonstrating the resulting degradation in P_{bit}. Only errors due to receiver noise are considered in the following analysis.

Figure 5.1 showed the variation of P_{bit} with E_c/N_o, the communication chip signal-to-noise ratio. The figure was computed under the assumption that the receiver has perfect synchronization. Errors in estimating the TOA of the synchronization signal prevent this from being the case. The following modifications to the formulas for P_{bit} have been derived in Appendix B. They show the average effect of this type of synchronization error on P_{bit}, assuming the error to be a Gaussian random variable of zero mean and variance σ^2.

$$\text{(PAM)} \qquad \overline{P_{bit}} \leq \exp\left[-\frac{E_c}{4N_o}\left(1 - \frac{\sigma^2 E_c}{8\tau_c^2 N_o}\right)\right], \tag{5-10}$$

$$\text{(DPSK)} \qquad \overline{P_{bit}} \leq \exp\left[-\frac{E_c/N_o}{1 + 8(\sigma^2/\tau_c^2)\, E_c/N_o}\right]. \tag{5-11}$$

We now replace σ^2 with the values that the lower bound to $\overline{\epsilon_t^2}$ takes on for large signal-to-noise ratios.

$$\text{(PAM)} \qquad \sigma^2 = \frac{0.1\,\tau_s^2}{(E_s/N_o)^2}, \tag{5-12}$$

$$\text{(DPSK)} \qquad \sigma^2 = \frac{t_r\,\tau_s}{4(E_s/N_o)}. \tag{5-13}$$

The above formulas have been derived in [22]. The corresponding values of $\overline{P_{bit}}$ are

$$\text{(PAM)} \qquad \overline{P_{bit}} \leq \exp\left[-\frac{E_c}{4N_o}\left(1 - \frac{1}{80\ E_c/N_o}\right)\right], \tag{5-14}$$

$$\text{(DPSK)} \qquad \overline{P_{bit}} \leq \exp\left[-\frac{E_c/N_o}{1 + 2(t_r/\tau_c)}\right]. \tag{5-15}$$

At signal-to-noise ratios large enough for reliable detection and estimation, these formulas show very small degradation in performance due to TOA estimation error. Thus, timing errors due to synchronization signal TOA estimation error will be neglected in the sequel.

5.6 DOWNLINK PERFORMANCE CURVES

N_d, the downlink capacity, has been computed for a variety of the signaling alternatives presented earlier in this section. These computations are summarized in parametric curves of capacity versus communication message length.

Figures 5.3 and 5.4 illustrate the variation of N_d, the downlink capacity, with the number of bits in the downlink communication message. Figure 5.3 assumes that the downlink signaling employs PAM while Figure 5.4 treats the case of DPSK modulation. Both figures display three curves corresponding to three different aircraft transponder front end noise figures; 15, 11, and 8 dB. Recall from the discussion in Section 3.3 that 15 dB is typical of the front end noise figure for a good ATCRBS transponder; 11 dB is

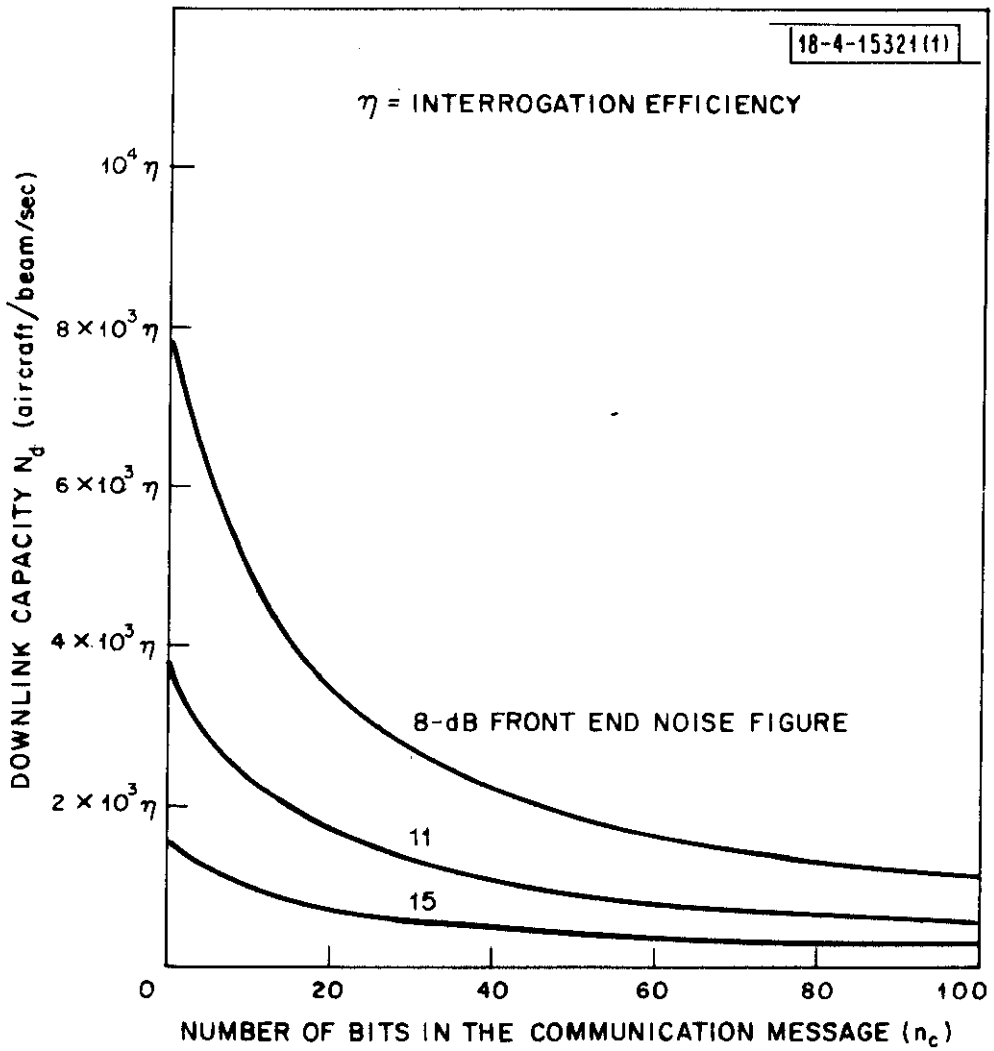

Figure 5.3. Downlink Capacity vs Number of Communication Message Bits for PAM Modulation.

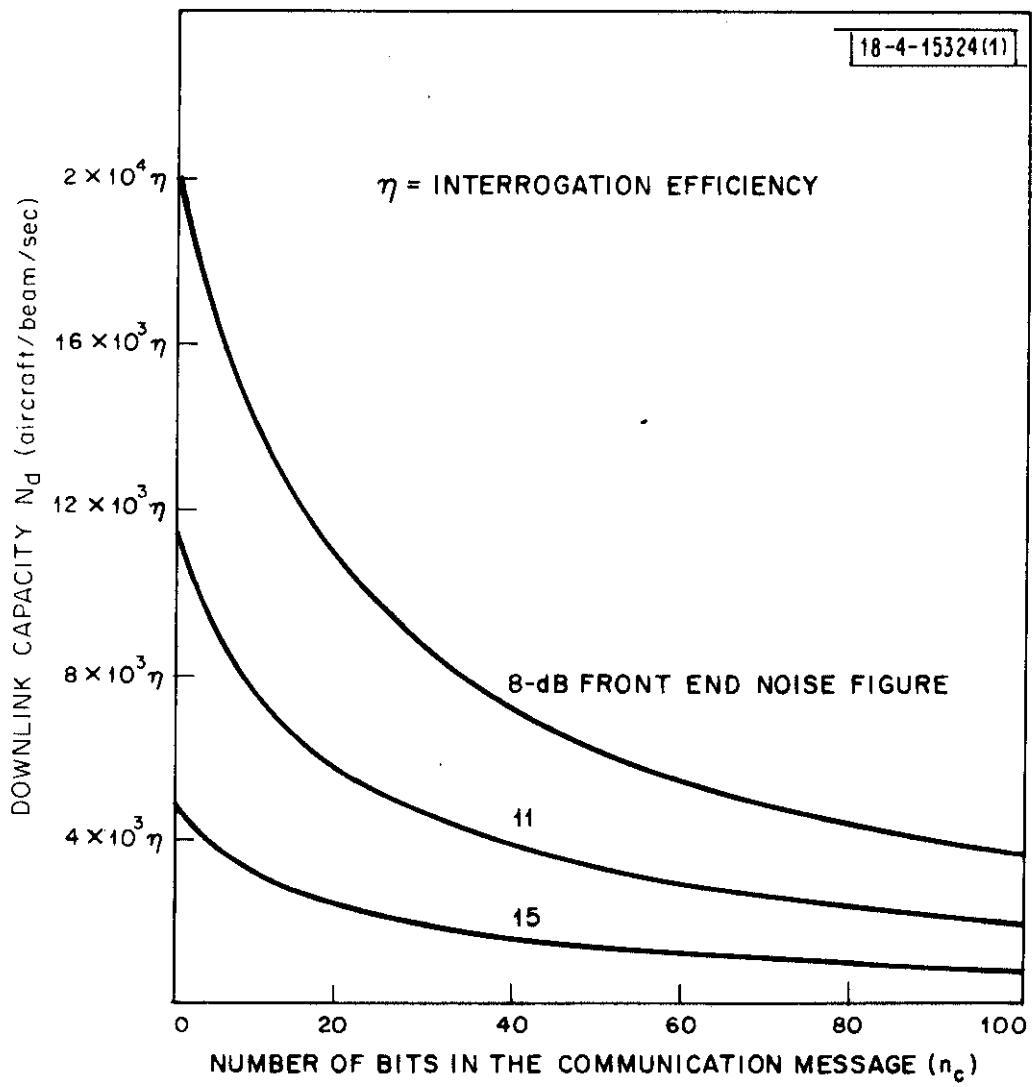

Figure 5.4. Downlink Capacity vs Number of Communication Message Bits for DPSK Modulation.

representative of the noise figure that can be achieved with moderate cost improvements in this transponder. A significant increase in cost is required to obtain the 8 dB front end noise figure.

It is illustrative to examine the downlink performance for a representative set of system parameters. Suppose we assume; (1) 20 bits per communication message, (2) an interrogation update period of 10 sec, i.e., the current ARSR update rate, (3) only 5 of the 10 satellite antenna beams required for CONUS coverage in simultaneous use and (4) an interrogation efficiency of 10%.*

Using these parameters, it is evident from the PAM results of Figure 5.3 that only 5,000 aircraft can be serviced with a 15 dB front end noise figure. The system service is doubled if the front end noise figure is 11 dB. The high cost front end noise figure (8 dB) will increase the service capacity to 18,000 aircraft. Thus, it is clear that for the chosen parameter values, PAM provides only a very limited downlink capacity.

Now consider the DPSK performance for these same parameter values. From Figure 5.4, service capacities corresponding to front end noise figures of 15, 11, and 8 dB are 13,000, 30,000 and 60,000 aircraft respectively. It is evident that the downlink capacity achievable with the moderate cost (11 dB) front end is interestingly large.

*The results of the analysis in Appendix E justify this as a conservative estimate of efficiency.

SECTION 6

UPLINK PERFORMANCE ANALYSIS

The performance of the aircraft-to-satellite uplink will now be examined by computing the uplink capacity N_u. We will show that as many as 30,000 aircraft can be reliably serviced by the uplink during a 10 sec update period provided the uplink signaling uses DPSK and the peak aircraft transmitter output power is 500 W. Such service also assumes a 10% interrogation efficiency and simultaneous operation of 5 satellite antenna beams. Problems associated with using PAM on the uplink will be explored.

The uplink capacity, N_u, is a function of the methods used to carry out the signaling on the aircraft-to-satellite link. Specifically, it depends upon the type of modulation employed, the ranging signal used and the method by which the uplink communication message is encoded. The choices considered in examining the uplink performance will be presented before the link capacity is computed.

6.1 MODULATION

Binary PAM and DPSK, the two modulation candidates considered in examining downlink performance, are also considered in examining uplink performance. Their binary error probability characteristics have been dealt with at length in Section 5.1. The modulation performance issues that arise relative to ranging signal design are discussed in Section 6.2.

Although performance is a factor to consider in the choice of modulation, cost is also a factor. The general aviation aircraft transponders in use today employ a binary PAM transmitter. For the same output power, a DPSK transmitter costs significantly more than a binary PAM transmitter. The cost increment was noted in Section 3.3 and is readily evident in comparing the two curves in Figure 3.5. The results indicate that DPSK transmitter costs for this application can be several times that of a binary PAM transmitter with the same output power. This cost differential precludes an immediate choice of modulation based solely upon efficient use of signal-to-noise ratio.

6.2 RANGING SIGNAL

The issues involved in choosing the uplink ranging signal are essentially the same as those associated with choosing the downlink synchronization signal. The principal difference lies in the more stringent accuracy requirement encountered on the uplink. The uplink ranging signal should provide an rms ranging error of less than 10 nsec to meet the position accuracy goal.

The type of uplink ranging signal is determined, to a great extent, by the choice of modulation. Binary PAM and DPSK each imply different ranging signal candidates. One candidate corresponding to each of these modulation possibilities is considered in examining uplink performance.

6.2.1 PAM Ranging Signal

The PAM ranging signal considered is a single square pulse. The ranging error, $\sqrt{\overline{\epsilon_t^2}}$, resulting from such a ranging signal can be computed by using (5-5) and the peak power-to-noise ratio given by the uplink power budget

of Table 4.... ... ranging error varies inversely with the transmitted power P_t (in kW):

$$\sqrt{\overline{\epsilon_t^2}} \geq \frac{40}{P_t} \quad \text{nsec} \quad . \tag{6-1}$$

Thus, a transmitter power of 500 W (the nominal value assumed in Table 4.2) implies a ranging error of 80 nsec. A transmitter power of at least 4 kW is required to reduce the ranging error to the desired 10 nsec. An uplink power of 4 kW would appear excessive for general aviation use. Thus, the uplink capacity will not be computed for PAM. It should be pointed out that there are other candidate PAM ranging signals, such as staggered pulse trains, which could possibly satisfy the ranging accuracy goal with a lower required peak power. Consideration of these signals is beyond the scope of this report. As will now be demonstrated, DPSK modulation can satisfy the ranging requirements; we shall restrict our further consideration to DPSK signaling schemes.

6.2.2 DPSK Ranging Signal

Binary phase coded signals with good autocorrelation properties are possible DPSK ranging signals. One of these, reported by Delong [25], is considered as the DPSK ranging signal candidate. This signal is composed of 85 chips and has a maximum normalized sidelobe magnitude of at most 0.08. It is assumed that each of the DPSK chips in the ranging signal has a 100 nsec duration and a 10 nsec rise time. The total signal duration is 8.5 μsec.

The rms TOA error, $\sqrt{\overline{\epsilon_t^2}}$, resulting from such a ranging signal has been obtained by Orr and Yates [22] and is illustrated as a function of signal-

to-noise ratio in Figure 6.1. The figure was computed assuming an a priori uncertainty interval width of 10 μsec. As an example, this might correspond to the maximum TOA uncertainty of an aircraft flying a known heading at a velocity less than 1000 ft/sec and being interrogated once every 10 sec. With the help of Table 4.2 the ranging signal-to-noise ratio is easily shown to be 15 dB. From Figure 6.1 it is found that $\sqrt{\epsilon_t^2} \simeq 10$ nsec. This satisfies the accuracy requirement in the definition of N_u.

6.3 COMMUNICATION MESSAGE ENCODING

The uplink communication message could be transmitted in either uncoded or coded format. For illustrative purposes, we examine only the uncoded format. This is not a necessary choice, but is made strictly to reduce the number of alternatives to be examined. It is desired that $P_{bit} < 10^{-6}$ on the uplink. Figure 5.1 indicates the chip signal-to-noise ratio required if this is to be achieved. By using this ratio with the uplink power budget, Table 4.2, it is easily shown that a 3.7 μsec DPSK chip is required.

6.4 UPLINK PERFORMANCE CURVES

The uplink capacity, N_u, will now be evaluated assuming the DPSK modulation for both the ranging signal and the communication message. N_u, is computed using the following formula

$$N_u = \frac{\eta}{T_s + (n_c + 2)\tau_c} \quad . \tag{6-2}$$

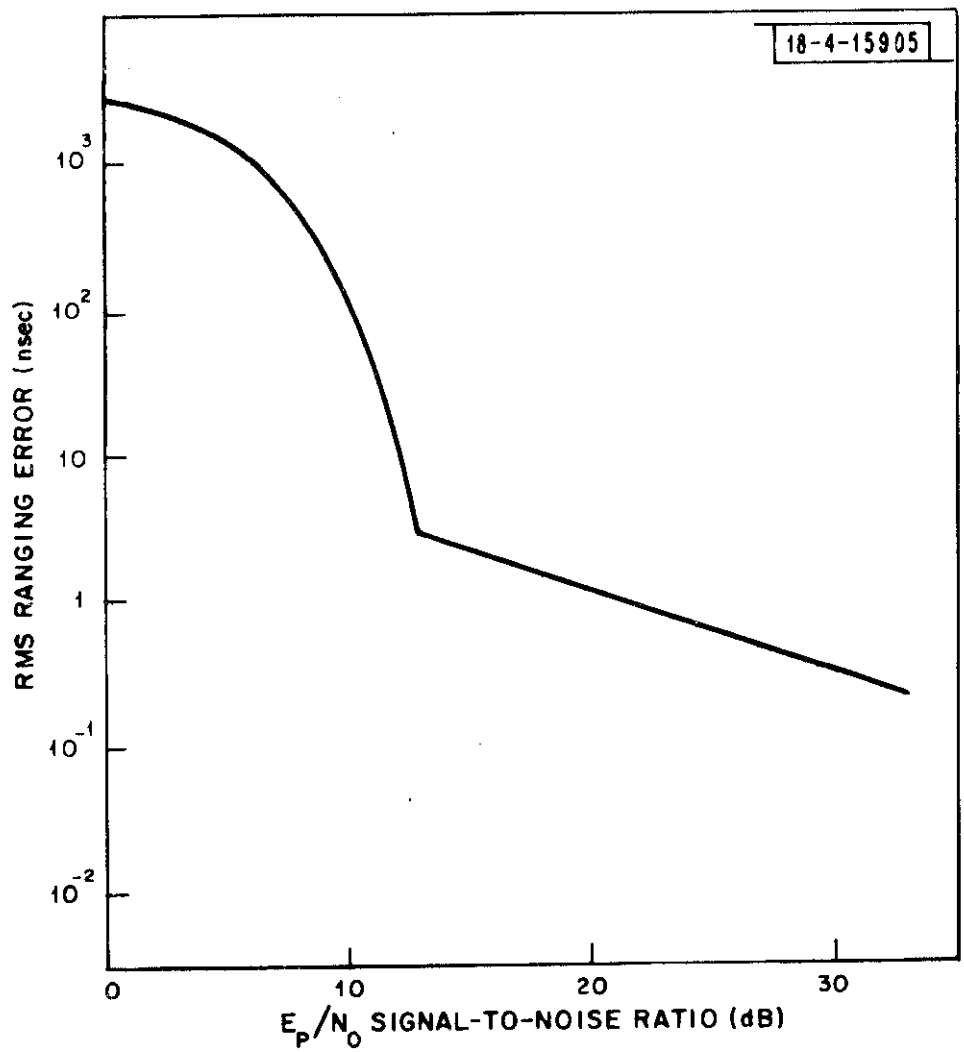

Figure 6.1. Uplink Ranging rms Error Due to Receiver Noise vs Signal-to-Noise Ratio for DPSK Modulation.

T_s is the duration of the ranging signal, 8.5 μsec, and n_c is the total number of communication bits transmitted on the uplink, including those that might be allotted for an optional uplink address.

Figure 6.2 illustrates N_u as a function of n_c for different transmitter peak powers.

The three curves illustrated in the figure correspond to transmitter powers of 250, 500, and 1000 W, of which the second is the nominal value in the power budget of Table 4.2. These curves can be used to draw some conclusions concerning uplink service. For illustrative purposes, suppose we assume the same system parameter values used to examine downlink performance; (1) 40 bits per communication message,* (2) an interrogation update period of 10 sec, (3) only 5 of the 10 antenna beams required for CONUS coverage in simultaneous use, and (4) an interrogation efficiency of 10%.

With these assumed parameter values, it is evident that when the peak transmitter power is 500 W, the uplink can service 35,000 aircraft with the required reliability. A 3 dB increase in power allows it to service 60,000 aircraft. A 3 dB decrease allows it to service 17,500 aircraft. It is interesting to note that these numbers roughly correspond to the number that can be serviced on the downlink at equivalent variations from the nominal receiver noise figure.

*This includes the 20 bits which might be allotted for the address.

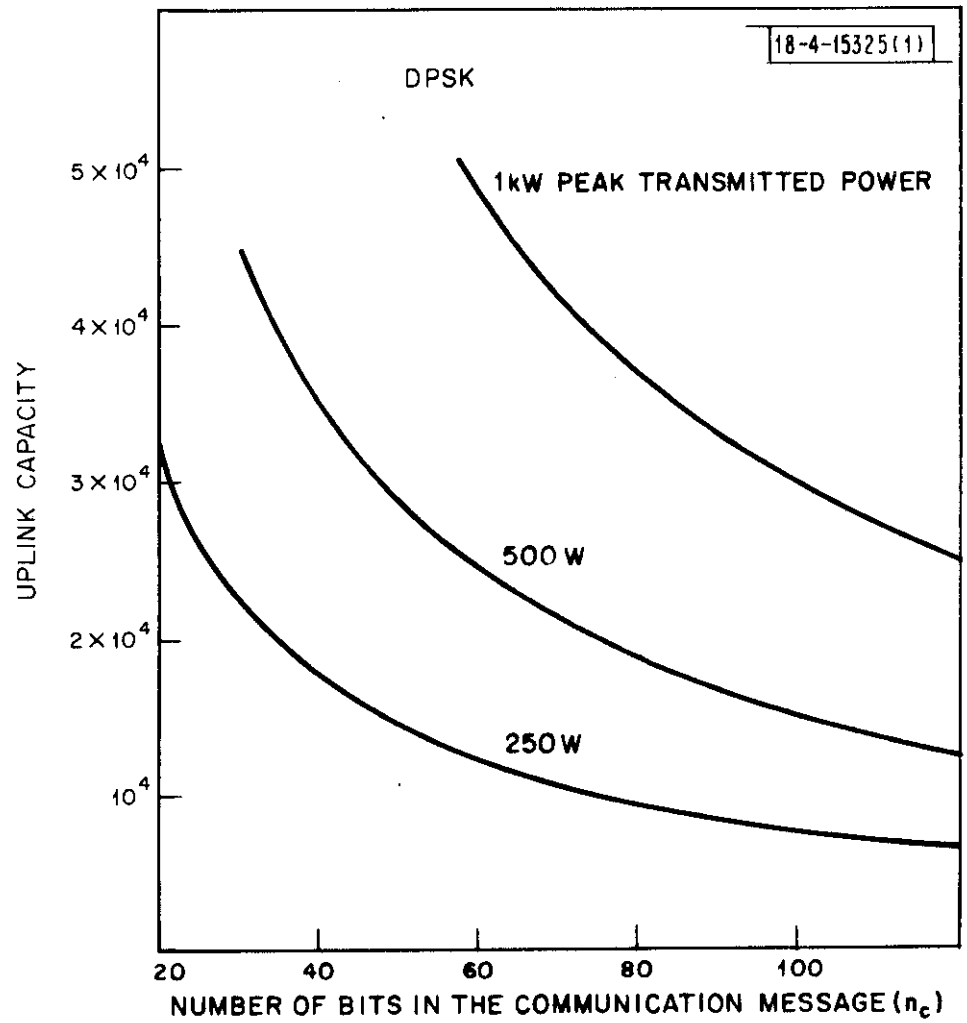

Figure 6.2. Uplink Capacity vs Number of Communication Message Bits for DPSK Modulation and Various Transmitter Powers.

6.5 POSITION MEASUREMENT ERROR

The rms position error is expressible as a product of two factors: the equivalent ranging error and the GDOP. The ranging error factor is the effective error in estimating the range between a satellite and an aircraft. The primary sources of ranging error are excess ionospheric delay, satellite ephemeris error, and TOA estimation error.* The exact values of these depend on satellite deployment, satellite tracking and calibration station implementation, satellite orbital parameters, the central processing facility, link characteristics (multipath, signal format, signal level, receiver noise, antenna gain, etc.), clock accuracy, etc.

For CAST, ionospheric errors can be kept within bound using a network of calibration stations employed to estimate the excess ionospheric time delay for use in correction of position determination data. For elevation angles in excess of 30°, the worst case** excess ionospheric ranging error is estimated to be 20 ft [26]. The satellite position is to be determined using satellite equations of motion (for an assumed geopotential model) to smooth satellite position data obtained from a network of tracking stations. The resulting effect on the ranging error term should be no more than 20 ft [5]. Errors in estimating the pulse TOA due to background noise, clock errors, non-optimum processors, etc., should not increase the overall rms ranging error to more than 40 ft.

---

* Ranging errors are proportional to TOA errors.

** During periods of high solar flux, near equinox and in early afternoon.

The GDOP is determined by the number and disposition of the satellites within view. Constellations which exhibit GDOP's ranging from 3 to 6 over CONUS are presented in Lee and Wade [13]. If such a constellation (e.g., the constellation discussed in Section 3.1) is employed, the resulting rms position measurement error is estimated to be in the vicinity of 120 ft. This resulting error value should be taken only as a guide and not as a firm system parameter. Determination of a refined estimate of the accuracy requires additional ionospheric data, a detailed system design for the tracking network and a more detailed analysis of the errors in the TOA estimation implementation.

SECTION 7

CRITICAL SYSTEM ISSUES

We complete this report on CAST with a brief discussion of two critical issues: the vulnerability to system jamming and the required computational facility. We shall demonstrate that; (1) the system can be disabled by a few low cost jammers, e.g., one 35 dBW ERP transmitter (30 W of RF power and a 20 dB gain, 17^{o} beamwidth antenna) per satellite antenna beam, and (2) in order to provide surveillance/communications service to 30,000 aircraft with a 10 second update rate, CAST requires a ground processing facility equivalent to several tens of present day general purpose CPU's and a large, fast, random access storage.

7.1 VULNERABILITY TO JAMMING

CAST is vulnerable to threats from terrestrial jammers. By merely transmitting a low power noise-like signal towards a satellite, a terrestrial jammer can completely disable the uplink beam channel within which he is located. We shall now evaluate the maximum required uplink jamming power, taking note that sophisticated jammers would require less power. It will be conservatively assumed that the jammer is transmitting a noise-like signal spread over a 20 MHz bandwidth (larger than the effective signal bandwidth), and that the effect at the receiver is equivalent to additive Gaussian noise which has a white spectrum across the band.

We shall assess the performance degradation due to such a jammer by determining the effect on the ranging error, $\sqrt{\epsilon_t^2}$. The DPSK ranging signal of Section 6.2.2 is assumed.

It was noted in Section 6.2.2 that if the synchronization signal energy-to-noise power density, E_s/N_o, is 15 dB, then $\sqrt{\epsilon_t^2}$ will be approximately 10 nsec, the specified goal. However, it is evident from Figure 6.1 that if E_s/N_o is reduced by 5 dB to a value of 10 dB, then the lower bound to $\sqrt{\epsilon_t^2}$ is in the threshold region where the error increases rapidly as E_s/N_o decreases. The ranging error will then be at least 100 nsec. This is unacceptably large for accurate position determination; hence, a satellite antenna beam channel having this large an error will be considered to be disabled.

Let us now compute the jammer ERP required in order to reduce E_s/N_o by 5 dB and thus disable an uplink beam channel. From Table 4.2 one notes that N_o = -201 dBW/Hz. If the jammer can transmit enough noise power to result in a jammer noise power density of -196 dBW/Hz at the satellite, then N_o will have been effectively increased by at least 5 dB and E_s/N_o will be effectively reduced by the same amount. Table 7.1 illustrates a power budget for such a jammer. The entries for path loss, peak satellite antenna gain and losses due to thermal distortion and shadowing are identical to the corresponding entries in the uplink power budget, Table 4.2. The jammer is assumed disadvantaged to the extent that he is located at the edge of one of the 3 dB satellite antenna beam footprints and suffers a loss due to satellite antenna shadowing. Table 7.1 indicates that a jammer ERP of 35 dBW will suffice. The cost of such a jammer should be less than that of the avionics needed to participate in the system.

Table 7.1. Jammer Power Budget.

Jammer ERP	35 dBW	
Path Loss	-192 dB	1600 MHz, 0.35 eccentricity
Peak Satellite Antenna Gain	42 dB	30 ft dish, 1600 MHz
Off Boresight Loss	-3 dB	Jammer at footprint edge
Thermal Distortion	-2 dB	
Antenna Shadowing	-1 dB	
Miscellaneous Losses	-2 dB	
Bandwidth	-73 dB-Hz	20 MHz bandwidth
Jammer Power Density (J)	-196 dBW/Hz	

Since 10 beams are used for CONUS coverage, it is estimated that jammers located at five places in CONUS could disable the entire system by jamming all 10 beams of one or more satellites. The colocated jamming facilities required for this task are certainly very inexpensive.

7.2 COMPUTATIONAL REQUIREMENTS

The use of satellites as a relay in a surveillance/communication link between aircraft over CONUS and ground-based installations has a concomitant requirement for centralized data processing. At the ground facility which receives the relayed transmissions, at least the following operations must be performed for each aircraft:

1. Detect ranging preamble.
2. Estimate TOA for each satellite in view.
3. Decode included message.
4. Precorrect TOA's for propagation delays.
5. Estimate aircraft position from TOA's.
6. Filter new position estimate with past position data.
7. Determine disposition of the data and route appropriately.
8. Reorder interrogation role and associated uplink messages.

In addition to the above, there are a variety of routine housekeeping functions, e.g., estimation of excess propagation delay map, tracking of satellite positions, system fault detection, etc.

A detailed assessment of the requisite computational requirements is beyond the scope of this report. We shall merely obtain a preliminary estimate of the computational load requirements for two functions; specifically, preprocessing of the received waveforms (1, 2 and 3 above) and position determination (5 above). These assessments are made in terms of present day computational standards, i.e., a 1 μsec cycle time CPU.

In order to provide the service claimed for the representative parameters of CAST (30,000 aircraft/10 sec), the processing of the signals received on one satellite-to-ground link must on the average be accomplished in less than 330 μsec. It is estimated that each satellite-to-ground link would require a single CPU to carry out TOA estimation, decoding and routing of the included message and routing of TOA data to the position determination processor. Ten CPU's would be required for a 10 satellite constellation.

Each aircraft position estimate requires certain TOA and satellite ephemeris data as input. In Appendix D it is shown that the equation for a least squares position estimate can be evaluated using approximately $(4N^2 + 14N + 42)$ multiplies and adds, where N is the number of satellites. In a computer for which floating point ADD and MULT are 2 and 10* cycle operations, respectively, the computation for a constellation in which 8 satellites are visible would take about 5 msec. Such a processor could handle about 200 aircraft/sec.

The above estimate of computation time is based upon the assumption that the reference point (a point in space near the aircraft about which the TOA equations are linearized) or the satellite position changes substantially from one position determination to the next. The effect of the linearization of the TOA equations has been studied, and it has been found that the reference point must be within 5 miles of the aircraft position in order to keep the linearization error somewhat less than 10 ft [27]. The sample interrogation algorithm given in Appendix E stipulates only that successively interrogated aircraft must be within 10 miles of one another. Thus, a given reference point is probably only valid for one or two successive estimates at best. Therefore, we assume that the indicated computation is required for each estimate.

The assumed 10 sec surveillance update interval could be subdivided into two separate 5 sec intervals, during which aircraft in 5 of the 10 satellite antenna beams could be interrogated. Real time data processing requires that

*A 10 cycle multiply is an estimate based on several present day machines.

the position estimates for the aircraft in one group of 5 beams be computed in half the update interval, i.e., 5 sec. A single CPU can handle 1,000 updates/ 5 sec. Maintenance of continual surveillance of 30,000 aircraft then requires at least 15 such units operating in parallel.

Hence, it is reasonable to expect that if the other computational requirements were included, then a total of several tens of CPU's would be required for real time processing and routing of data.

APPENDIX A

LINEAR CODES FOR DISCRETE ADDRESS TRANSMISSION

In Section 5 of this report, linear algebraic codes are considered as address sets for the downlink. Derivations of upper bounds to the miss and false alarm probabilities (P_M and P_F) associated with such address sets are given in this Appendix. The derivation is prefaced by a general discussion of the properties and nomenclature associated with linear codes.

A.1 LINEAR CODES

Let A_m be the set of all binary sequences of length m. For any integers n (called the block length) and k, such that $n \geq k$, a binary (n, k) code is a one to one mapping, $\Phi(\cdot)$, of A_k into A_n. The sets A_k and $\Phi(A_k)$ are called the message and codeword sets, respectively. Each of the 2^k codewords in $\Phi(A_k)$ can be uniquely decoded to its corresponding message word since $\Phi(\cdot)$ is a one to one mapping.

If $\Phi(\cdot)$ is a linear transformation the code is called a linear code.

When a codeword from a binary (n, k) code is transmitted over a binary communication channel, there is the possibility that some of the digits will be received in error. This, in turn, may cause the codeword to be decoded in error. If the channel is a memoryless binary symmetric channel (BSC),* there is an optimum procedure for deciding which codeword was sent,

*The memoryless BSC is a channel in which received digit errors occur independently with equal probability (p); the error probability is independent of the transmitted digit.

given the channel output word. This "decoding rule" is based upon the distance between a pair of codewords. This is now defined. Let $\underline{a} = a_1 a_2 \ldots a_n$ and $\underline{b} = b_1 b_2 \ldots b_n$ be two binary codewords. The Hamming distance between $\underline{a}$ and $\underline{b}$ is defined as

$$d(\underline{a}, \underline{b}) = \sum_{i=1}^{n} \delta^{\dagger}(a_i, b_i) \tag{A-1}$$

where $\delta^{\dagger}(\cdot, \cdot)$ is the Kronecker delta function

$$\delta^{\dagger}(x, y) = \begin{cases} 0 & ; \quad x = y \\ 1 & ; \quad x \neq y \end{cases} . \tag{A-2}$$

If the following decoding rule is used, the probability that a received channel word will be decoded incorrectly is minimized. Let $\underline{a}$ be a received channel word. Decode $\underline{a}$ as a word $\underline{b} \in \Phi(\cdot)$ such that

$$d(\underline{a}, \underline{b}) = \min_{x \in \Phi(\cdot)} d(\underline{a}, \underline{x}) . \tag{A-3}$$

In words, if $\underline{a}$ is received, decide that the codeword of Φ was transmitted which is closest in Hamming distance to $\underline{a}$.

The minimum distance, d, of a code is defined as

$$d = \min_{\substack{\underline{a},\underline{b} \in \mathcal{P}(A_k) \\ \underline{a} \neq \underline{b}}} \{d(\underline{a},\underline{b})\} \quad . \tag{A-4}$$

The maximum number of digit errors that may occur in the transmission of a codeword without causing the minimum distance rule to incorrectly decode the received word is called the error correcting capacity of the code. This parameter is denoted by t and is given in terms of the minimum distance:

$$t = \begin{cases} (d/2) - 1 & ; \quad d \text{ even} \\ (d-1)/2 & ; \quad d \text{ odd} \end{cases} \quad . \tag{A-5}$$

With respect to the CAST address set problem, we are interested in linear codes for which $k \geq 20$, since each aircraft address must represent 20 bits of information. An enumeration of all linear codes of odd block length $n \leq 65$ is provided in Appendix D of Peterson and Weldon [28]. From their tabulation, three codes, each having k=20, are chosen as candidates examined in Section 5. Each of these codes has the largest value of d for its block length. The parameters of these codes are given in Table A.1. The first of these cases is actually the uncoded case considered in Section 5 in which the message words and the codewords are one and the same.

Table A.1. Parameters of Address Set Candidates.

n	k	d	t
20	20	1	0
31	20	6	2
41	20	10	4

A.2 UPPER BOUNDS TO P_M AND P_F

It is assumed that an (n, k) linear code with minimum distance d is used as an address set for the CAST satellite-to-aircraft link. This link may be treated as a binary symmetric channel. Its crossover probability, which is a function of the modulation and the received signal-to-noise ratio, is designated as p. This description allows the downlink addressing technique to be expressed entirely in the nomenclature of linear coding theory and to be studied in that context. Upper bounds to the miss and false alarm probabilities for the address set are derived in the sequel.

A.2.1 Problem Formulation

The following abstract description of the downlink addressing problem is used as a basis for the succeeding analysis. A word is chosen from an (n, k) code and is transmitted over a binary symmetric channel having crossover probability p. The receiver wishes to determine whether the transmitted sequence is a certain codeword (his own "address"). He decides that it is if

the Hamming distance between the received sequence and his address does not exceed a threshold T, which is assumed to be less than the minimum distance d. This procedure is repeated until all words of the code (or a designated subset of them) have been transmitted.

Two distinct error events are associated with this process. It is important to emphasize that the sample space over which these events are defined is the transmission of a subset of distinct codewords (called a roll call), and not merely a single transmission. The first error event is a "miss." This is the event which occurs when the receiver fails to correctly decode the transmission of his own address. This event may be statistically characterized over the smaller sample space of a single transmission, since no codeword is transmitted more than once. The second error event is a "false alarm." This is said to occur if, during the transmission of the codeword subset, the receiver at least once erroneously decodes some received word as his address codeword. The original sample space is required to characterize a false alarm.

A.2.2 Probability of Miss - P_M

From the definition of miss and the assumed decoding rule it is clear that miss occurs if and only if the distance between the transmitted and received words exceeds the threshold T. For this to occur, at least T digits must be received in error. The probability of exactly j channel errors is a binomial random variable, and hence the miss probability is

$$P_M = \sum_{j=T+1}^{n} \binom{n}{j} p^j (1 - p)^{n-j} \quad . \tag{A-6}$$

An upper bound to P_M can be obtained by noting that if $T > np$, then the $j = T + 1$ term is the maximum term in the sum. When this is the case, all summands may be replaced by the maximum term and the resulting bound is

$$P_M \leq (n - T) \binom{n}{T+1} p^{T+1} (1 - p)^{n-(T+1)} \quad . \tag{A-7}$$

The condition $T > np$ corresponds to the situation on the downlink.

A.2.3 Probability of False Alarm Per Transmission

Prior to computing P_F, it is necessary to calculate the conditional probability that a false alarm occurs on a single transmission, given the distance between the transmitted word and the receiver address.

It is sufficient to consider the set of words shown in Table A.2, in which the transmitted sequence $\underline{X}$ contains δ ones and $(n-\delta)$ zeros and the aircraft address is assumed to be the $\underline{0}$ word. A false alarm occurs if a received word has weight (distance to the $\underline{0}$ word) $\leq T$.

Table A.2. Codewords For False Alarm Analysis.

Transmitted Word	=	$\underline{X}$	=	1	1	.	.	.	1	0	0	.	.	.	0
All-Zero Word	=	$\underline{0}$	=	0	0	.	.	.	0	0	0	.	.	.	0
Received Word	=	$\underline{R}$	=	1	0	.	.	.	1	0	1	.	.	.	0
					δ digits					$(n-\delta)$ digits					

As a first step, the probability that $d(\underline{R}, \underline{0}) = d_o$ (the distance between $\underline{R}$ and $\underline{0}$ is d_o) is calculated. If j transmitted zeros are received in error, the weight of $\underline{R}$ will be d_o only if $(\delta - d_o + j)$ transmitted ones are received in error. Since only δ ones are transmitted, j cannot exceed d_o. Neither can it exceed the number of transmitted zeros, $(n-\delta)$. The probability of this event is

$$\left\{\binom{n-\delta}{j} p^j (1-p)^{n-\delta-j}\right\} \cdot \left\{\binom{\delta}{\delta-d_o+j} p^{\delta-d_o+j} (1-p)^{d_o-j}\right\}$$

$$\Updownarrow \qquad\qquad \Updownarrow$$

Prob $\{$j 0's received in error$\}$ Prob $\{(\delta-d_o+j)$ 1's received in error$\}$

The possible ways of arriving at $d(\underline{R}, \underline{0}) = d_o$ are exhausted by letting j range over $[0, \min(d_o, n-\delta)]$:

$$\text{Prob}\{d(\underline{R}, \underline{0}) = d_o\} = \sum_{j=0}^{\min(d_o, n-\delta)} \binom{n-\delta}{j} \binom{\delta}{d_o-j} p^{\delta-d_o+2j} (1-p)^{n-(\delta-d_o+2j)} .$$

(A-8)

The probability that a false alarm will occur on a single transmission when the transmitted word is at distance δ from the receiver address is $P_{f|\delta}$:

$$P_{f|\delta} = \text{Prob}\{d(\underline{R}, \underline{0}) \leq T\}$$

$$= \sum_{d_0=0}^{T} \sum_{j=0}^{\min(d_o, n-\delta)} \binom{n-\delta}{j}\binom{\delta}{d_o-j} p^{\delta-d_o+2j} (1-p)^{n-(\delta-d_o+2j)} .$$

(A-9)

Equation (A-9) cannot be easily simplified, but it can be upper bounded using the following argument. Let $a_j(d_o)$ represent the summand in (A-9); the ratio

$$\frac{a_{j+1}(d_o)}{a_j(d_o)} = \frac{(n-\delta-j)(d_o-j)}{(j+1)(\delta-d_o+j+1)} \left(\frac{p}{1-p}\right)^2 \qquad \text{(A-10)}$$

decreases with increasing j and is < 1 for all j as long as $p \ll 1/\sqrt{nd_o}$. Under these assumptions, the j=0 term is maximum for any d_o. This term corresponds to the case in which none of the $(n-\delta)$ transmitted zeros are received in error, and therefore the received word weight d_o cannot exceed the transmitted weight δ. Replacement of all the j terms in (A-9) by the j=0 term yields

$$P_{f|\delta} \leq \sum_{d_o=0}^{T} [1 + \min(d_o, n-\delta)] \binom{\delta}{d_o} p^{\delta-d_o}(1-p)^{n-(\delta-d_o)} \quad . \qquad \text{(A-11)}$$

In order to further bound $P_{f|\delta}$, the ratio test with respect to d_o is performed (with j fixed at 0):

$$\frac{a_o(d_o)}{a_o(d_o-1)} = \frac{\delta+1-d_o}{d_o} \left(\frac{1-p}{p}\right) > \frac{d+1-T}{T} \left(\frac{1-p}{p}\right) \quad . \qquad \text{(A-12)}$$

This ratio is always greater than 1 as long as $p \ll (d+1-T)/T$, in which case the $d_o = T$ term dominates the sum in (A-11). This observation permits the following bound on $P_{f|\delta}$:

$$P_{f|\delta} \leq \frac{(T+1)(T+2)}{2} \binom{\delta}{T} p^{\delta-T}(1-p)^{n-(\delta-T)};\ p \ll 1/\sqrt{nT} \quad . \tag{A-13}$$

The condition on the above bound is not severe and is satisfied by parameter values considered for the CAST application.

A.2.4 Probability of False Alarm Per Roll Call - P_F

The probability that at least one false alarm occurs in a roll call can now be calculated in terms of $P_{f|\delta}$. Let N_δ be the number of words at distance δ from a given codeword (if the code is a linear code, this number is not a function of the codeword). The probability that no false alarms are generated by words at distance δ is $(1-P_{f|\delta})^{N_\delta}$. Over a roll call which includes the full code,

$$P_F = 1 - \prod_{\delta=d}^{n} (1-P_{f|\delta})^{N_\delta} \quad . \tag{A-14}$$

The following easily verified steps are used to overbound P_F:

$$\begin{aligned} P_F &\leq 1 - \prod_{\delta=d}^{n} (1-N_\delta P_{f|\delta}) \\ &\leq 1 - \left[1 - \sum_{\delta=d}^{n} N_\delta P_{f|\delta}\right] \\ &= \sum_{\delta=d}^{n} N_\delta P_{f|\delta} \quad . \end{aligned} \tag{A-15}$$

From (A-13) it is obvious that P_F is dominated by the "nearest neighbor" false alarm term, $P_{f|d}$, when the crossover probability p is small. Replacing $P_{f|\delta}$ by $P_{f|d}$ yields the bound

$$P_F \leq \left(\sum_{\delta=d}^{n} N_\delta \right) P_{f|d}$$

$$\leq 2^k P_{f|d} \quad . \tag{A-16}$$

However, if it is true that

$$P_{f|d} \gg P_{f|\delta} \quad ; \quad \delta > d \tag{A-17}$$

then it is more accurate to retain only the $\delta=d$ term in (A-15), leading to

$$P_F \simeq N_d P_{f|d} \quad . \tag{A-18}$$

The number of words of weight d is upper bounded by $N_d \leq \binom{n}{d}$; introducing this into (A-16) yields the desired upper bound,

$$P_F \lesssim \frac{(T+1)(T+2)}{2} \binom{n}{d} \binom{d}{T} p^{d-T} \quad . \tag{A-19}$$

In (A-19) the terms in (1-p) have been neglected.

In the uncoded case (n=k, d=1, T=0), (A-19) is a strict upper bound which reduces to

$$P_F \leq kp \quad . \tag{A-20}$$

A.2.5 Choice of Threshold

The bounds obtained thus far depend on the decoding threshold T as follows:

$$P_M \propto p^{T+1} \; ; \qquad P_F \propto p^{d-T} \; . \tag{A-21}$$

In order to keep both P_M and P_F small for some fixed p, both (d-T) and (T+1) should be large. The ideal compromise choice for T is the error correcting capacity t defined in Section A.1, whose value is essentially d/2. For this choice, the exponential dependence of P_M and P_F upon p is as follows:

d even	d odd
$P_M \propto p^{d/2}$	$P_M \propto p^{(d+1)/2}$
$P_F \propto p^{d/2+1}$	$P_F \propto p^{(d+1)/2}$

For codes whose minimum distance is even, P_F can be made smaller than P_M by a factor proportional to p; this is to be contrasted with the uncoded case in which P_M and P_F have similar p-dependence. For other choices of T, one of P_M and P_F is emphasized at the expense of the other; the corresponding address ROC's are considerably different than those which result from the choice T = t.

APPENDIX B

THE DEPENDENCE OF P_{bit} ON SYNCHRONIZATION ERROR

In this Appendix, modifications to the formulas for the binary error probability P_{bit} will be derived which take into account receiver synchronization error. Both PAM and DPSK modulation will be considered. For each of these modulations the following probabilities are computed: (1) $P_{bit}(\Delta t)$, the conditional probability of error for the optimum demodulation in the presence of a given synchronization error; (2) $\overline{P_{bit}}$, the average probability of error assuming that the synchronization errors are random and have a Gaussian distribution.

The results for $P_{bit}(\Delta t)$ are used to compute the effects of clock and relative motion errors. Those for $\overline{P_{bit}}$ are used to compute the effect of error in the estimate of the synchronization signal TOA.

B.1 EFFECT OF SYNCHRONIZATION ERROR ON PAM

The processing which minimizes the PAM chip error probability (in the absence of synchronization error) consists of matched filtering the chip waveform and performing a threshold test on a sample of the filter output envelope. The sample is taken at the time of the trailing edge of the input pulse. The optimum threshold setting is a function of the a priori probabilities of the "off" and "on" signals (they are assumed to be equiprobable here), the received signal energy and the noise power density.

The error probability which is achieved by the PAM receiver is a function only of the signal-to-noise ratio in the output sample. When the signal is present and the sample is improperly timed, the signal-to-noise ratio is degraded; the degradation is linear over the duration of the signaling chip. Thus for a chip of duration τ, an error of Δt in synchronization increases the error probability to approximately

$$P_{bit}(\Delta t) = \frac{1}{2} \exp\left[- \frac{E_c}{4N_o} \left(1 - \frac{|\Delta t|}{\tau} \right) \right] \; ; \; |\Delta t| < \tau \quad . \tag{B-1}$$

The synchronization error may be viewed as an additional loss factor of $10 \log_{10}(1-|\Delta t|/\tau)$ dB in the link power budget.

Now assume that Δt is a zero mean Gaussian random variable of variance σ^2,* and compute the average error probability due to synchronization error. The expectation of (B-1) is taken with respect to Δt:

$$\overline{P_{bit}} = E_{\Delta t}[P_{bit}(\Delta t)] = \frac{1}{\sqrt{2\pi\sigma^2}} \int_{-\infty}^{\infty} d(\Delta t)\, 1/2 \exp\left[- \frac{E_c}{4N_o} \left(1 - \frac{|\Delta t|}{\tau} \right) - \frac{(\Delta t)^2}{2\sigma^2} \right]$$

$$= 1/2 \exp\left[- \frac{E_c}{4N_o} \right] \frac{1}{\sqrt{2\pi\sigma^2}} \left\{ \int_{-\infty}^{0} dx \exp\left[- \frac{x^2}{2\sigma^2} - \frac{E_c x}{4N_o} \right] \right.$$

$$\left. + \int_{0}^{\infty} dx \exp\left[- \frac{x^2}{2\sigma^2} + \frac{E_c x}{4N_o} \right] \right\} \quad . \tag{B-2}$$

*This assumption is consistent with the large signal-to-noise ratio asymptotic behavior of a maximum likelihood estimate of Δt.

Each of the integrals in the latter step of (B-2) can be evaluated in terms of the Gaussian error integral

$$\Phi(\alpha) = \frac{1}{\sqrt{2\pi}} \int_{\alpha}^{\infty} dy \exp\left[-\frac{y^2}{2}\right] \tag{B-3}$$

by completing the square in x. The result of carrying out the indicated calculation is

$$\overline{P_{bit}} = \left[1 - \Phi\left(\frac{\sigma E_c}{4N_o\tau}\right)\right] \exp\left[-\frac{E_c}{4N_o}\left(1 - \frac{\sigma^2 E}{8 N_o \tau^2}\right)\right] . \tag{B-4}$$

Since $\Phi(\cdot)$ is non-negative, (B-4) is upper bounded by

$$\overline{P_{bit}} \leq \exp\left[-\frac{E_c}{4N_o}\left(1 - \frac{\sigma^2 E_c}{8 N_o \tau^2}\right)\right] . \tag{B-5}$$

B.2 EFFECT OF SYNCHRONIZATION ERROR ON DPSK

Figure 3.7 illustrates a block diagram of one realization of a DPSK demodulator which is optimum in the absence of synchronization error. The received DPSK chips are matched filtered and then supplied to the chip delay and multiply circuit. This operation extracts the data from the relative phase information in adjacent chips. The IF second harmonic generated in the multiplier and any residual carrier are eliminated by the subsequent lowpass filter. The resultant lowpass signal is sampled at the trailing edge time of each chip, and the information is decoded by a polarity test on the sequence of samples.

In order to assess the effects of synchronization error on the reliability of the DPSK decoding, the demodulator output waveforms in the absence of noise must be considered. Figure B.1 shows the outputs for the four possible combinations of adjacent phase differentials in the received signals. The output signal decreases from its peak value most rapidly as a function of synchronization error in the case in which there are two adjacent phase reversals in the input. This decrease is a parabolic function.

Since the demodulator is a nonlinear system the noise output is signal dependent and nonstationary. However, by assuming that the output noise variance is constant at its maximum value we will overbound its effect on P_{bit}. The maximum value can be shown to occur at the intended sampling instant.

By combining the two previous arguments we find the following upper bound to $P_{bit}(\Delta t)$:

$$P_{bit}(\Delta t) \leq \frac{1}{2} \exp\left[-\frac{E_c}{N_o}\left(1-2\frac{|\Delta t|}{\tau}\right)\right]; \quad \Delta t \leq \frac{\tau}{2} \quad . \tag{B-6}$$

For $\Delta t \ll \tau$, the effect is essentially equivalent to a loss of $10 \log_{10}(1-4|\Delta t|/\tau)$ dB in chip signal-to-noise ratio. If, once again, it is assumed that Δt is Gaussian with zero mean and variance σ^2, then (B-6) can be averaged with respect to Δt to yield an upper bound on the average chip error probability $\overline{P_{bit}}$.

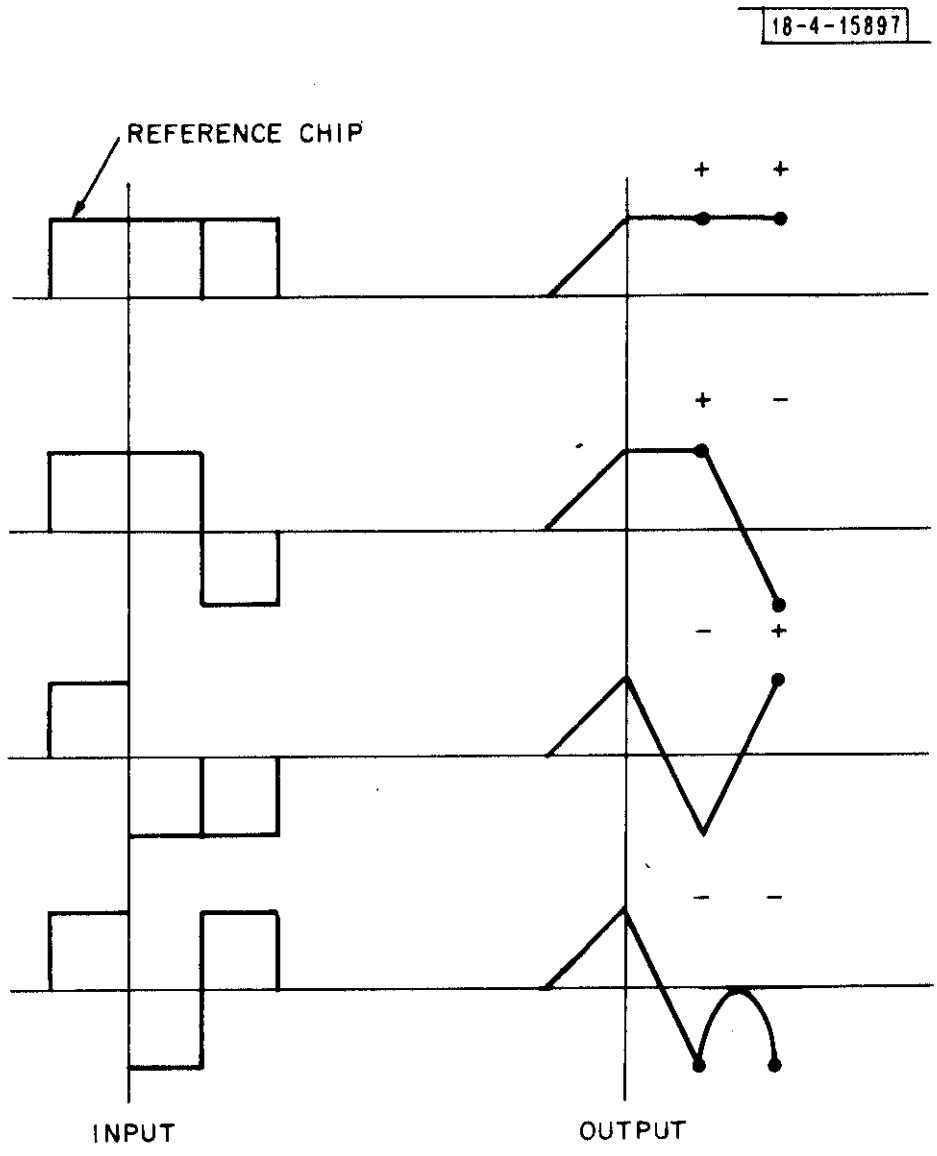

Figure B.1. DPSK Demodulator Inputs and Outputs.

$$\overline{P_{bit}} = \frac{1}{\sqrt{2\pi\sigma^2}} \int_{-\infty}^{\infty} d(\Delta t)\, \frac{1}{2} \exp\left[-\frac{E_c}{N_o} \left(1 - 2\,\frac{|\Delta t|}{\tau}\right)^2 - \frac{(\Delta t)^2}{2\sigma^2} \right]$$

$$= \frac{1}{\sqrt{2\pi\sigma^2}} \int_{0}^{\infty} dx \exp\left[-\frac{E_c}{N_o} \left(1 - \frac{2x}{\tau}\right)^2 - \frac{x^2}{2\sigma^2} \right] \quad . \qquad \text{(B-7)}$$

Completion of the square in the integrand exponent leads to the evaluation of the latter integral in (B-7):

$$\overline{P_{bit}} \leq \frac{1 - \Phi\left(\dfrac{4\sigma\, E_c/N_o}{\sqrt{1 + 8\sigma^2\, E_c/N_o}} \right)}{\sqrt{1 + 8(\sigma^2/\tau^2)\, E_c/N_o}} \exp\left[-\frac{E_c/N_o}{1 + 8(\sigma^2/\tau^2)\, E_c/N_o} \right] \quad . \qquad \text{(B-8)}$$

The coefficient of the exponential term in (B-8) is ≤ 1, so that $\overline{P_{bit}}$ may be further bounded:

$$\overline{P_{bit}} \leq \exp\left[-\frac{E_c/N_o}{1 + 8(\sigma^2/\tau^2)\, E_c/N_o} \right] \quad . \qquad \text{(B-9)}$$

APPENDIX C

COMPUTATION OF DOWNLINK CAPACITY

In this Appendix the relation between the downlink capacity (N_d) and the downlink signal durations is established. The effects of timing error are taken into account and it is shown how to choose the resynchronization period to maximize N_d. A calculation of N_d is carried out for one set of parameter values assuming DPSK demodulation. The derivation for PAM is similar.

Notation

x = Resynchronization Period

T_s = Duration of Synchronization Signal

τ_a = Duration of Address Chip

τ_c = Duration of Communication Chip

n_a = Number of Address Chips

n_c = Number of Communication Chips

η = Interrogation Efficiency

δ = Maximum Timing Error/sec

T_{tot} = Signal Duration per Aircraft in the Absence of Timing Errors

Capacity Formula

During the resynchronization period, the time available for downlink signaling is $\eta(x-T_s)$ sec. In the absence of any timing errors only

$$T_{tot} = (n_a+1)\tau_a + (n_c+1)\tau_c \text{ sec}^* \qquad (C-1)$$

are required to interrogate each aircraft. Compensation for clock and relative motion error is achieved by increasing the chip lengths and the resulting total signal duration.

In Appendix B it was shown that a timing error of ϵ sec in demodulation of a DPSK chip reduces the effective signal-to-noise ratio in the chip by at most a factor of $(1-4|\epsilon|/\tau)$, $|\epsilon| \ll \tau$. If the chip duration is adjusted to a value τ'

$$\tau' = \tau+4|\epsilon| \qquad (C-2)$$

then the adjusted chip will have at least the same signal-to-noise ratio as the original chip in the absence of timing error. Since there are a total of (n_a+n_c+2) chips in the signal, the adjusted value of the total duration per signal, T'_{tot}, is

$$T'_{tot} = T_{tot} + 4(n_a+n_c+2)|\epsilon| \quad . \qquad (C-3)$$

The maximum timing error which can occur over a resynchronization period is

$$\epsilon = \delta(x-T_s) \qquad (C-4)$$

---

*The number of chips n_a and n_c are increased by one to include the DPSK reference chip. For PAM signaling this additional chip may be omitted.

since δ is the maximum per second drift in the timing reference. The number of aircraft serviced per beam per resynchronization period is

$$\frac{\eta(x-T_s)}{T_{tot} + 4(n_a+n_c+2)\,\delta\,(x-T_s)} \quad .$$

If this is divided by x, it equals N_d:

$$N_d(x) = \frac{\eta\,(x-T_s)}{x\left[T_{tot} + 4(n_a+n_c+2)\,\delta\,(x-T_s)\right]} \quad . \tag{C-5}$$

This function can be optimized with respect to x for $x > T_s$: the result is that the optimum resynchronization period, $\tilde{x}$, is

$$\tilde{x} = T_s\left[1 + \sqrt{\frac{T_{tot}}{4(n_a+n_c+2)\,\delta\,T_s}}\right] \quad \text{sec} \tag{C-6}$$

and the corresponding optimum value of N_d is

$$N_d(x) = \frac{\eta/T_{tot}}{\left[1 + \sqrt{\frac{4(n_a+n_c+2)\,\delta\,T_s}{T_{tot}}}\right]^2} \quad \text{aircraft} \, . \tag{C-7}$$

The result shows how the capacity degrades from the error-free value η/T_{tot} as δ increases.

Computation of N_d

Equations (C-6) and (C-7) are now evaluated for the following case:

$T_s = 40\ \mu\text{sec}$

$\tau_a = 2.3\ \mu\text{sec}$

$\tau_c = 4.2\ \mu\text{sec}$

$n_a = 31$ chips

$n_c = 20$ chips

$\eta = 0.1$

$\delta = 10^{-6}$

The results are

$$\tilde{x} = 5.56 \text{ msec} \tag{C-8}$$

$$N_d(\tilde{x}) = 609 \text{ aircraft/beam/sec} \ . \tag{C-9}$$

APPENDIX D

COMPUTATION OF THE HYPERBOLIC MULTILATERATION EQUATION

Lee [29] has analyzed hyperbolic multilateration methods for aircraft position determination, and has shown that when the TOA errors at the satellites are equivariant, the equation by which the estimated position, ΔR^*, of an aircraft is computed is as follows:

$$\underline{\Delta R}^* = [F'H'(HH')^{-1} H F]^{-1} F'H'(HH')^{-1} [c\underline{\Delta T} - H\underline{R}] \qquad (D\text{-}1)$$

in which:

$\underline{\Delta R}^*$ = The aircraft position vector estimate relative to a reference point near the aircraft

F = An N x 3 matrix whose components depend upon both the reference point and the satellite positions

N = Number of satellites

H = An (N-1) x N matrix whose components are constants

c = Speed of light

$\underline{\Delta T}$ = An N-1 dimensional vector of differential arrival times

$\underline{R}$ = An N dimensional vector of ranges from the reference point to the satellites

The equation can be put in the following form which is more suitable for computation:

$$\underline{\Delta R}^{*} = L^{-1}[cF'H'(HH')^{-1}\,\underline{\Delta T} - K'\underline{R}] \qquad (D\text{-}2)$$

in which

$$L = K'K \qquad (D\text{-}3)$$

$$K = H'(HH')^{-1}\,HF \quad . \qquad (D\text{-}4)$$

In the following, we calculate the number of additions and multiplications required to evaluate (D-2) on the assumption that the matrix H (and functions of H) may be precomputed and stored. Thus $\underline{\Delta T}$, $\underline{R}$, and F are treated as the inputs to the equation.

The following analysis depends strongly upon the simple fact that the product of two matrices whose (row x column) dimensions are (A x B) and (B x C) can be computed using approximately ABC multiplications and additions.

A reasonably efficient way to evaluate (D-2) is outlined below; the number of operations required to compute each step is tabulated.

Matrix	Dimensions	Number of Operations		
$K = [H'(HH')^{-1} H] F$	$\underbrace{(N\times N)\ (N\times 3)}_{(N\times 3)}$	$3N^2$		
$L = K'K$	$\underbrace{(3\times N)\ (N\times 3)}_{(3\times 3)}$		$9N$	
L^{-1}	(3×3)			30^*
$[H'(HH')^{-1}]\ \underline{\Delta T}$	$\underbrace{[N\times(N-1)]\ [(N-1)\times 1]}_{(N\times 1)}$	N^2	$-N$	
$F'[H'(HH')^{-1}\ \underline{\Delta T}]$	$\underbrace{(3\times N)\ (N\times 1)}_{(3\times 1)}$		$3N$	
$K'\underline{R}$	$\underbrace{(3\times N)\ (N\times 1)}_{(3\times 1)}$		$3N$	
$cF'H'(HH')^{-1}\ \underline{\Delta T} - K'\underline{R}$	(3×1)			3
$L^{-1}[cF'H'(HH')^{-1}\ \underline{\Delta T} - K'\underline{R}]$	$\underbrace{(3\times 3)\ (3\times 1)}_{(3\times 1)}$			9
Total		$4N^2 + 14N + 42$		

*This figure upper bounds the number of operations required to compute the determinant by the method of cofactors.

APPENDIX E

INTERROGATION SCHEDULING

The issues involved in interrogation scheduling for CAST have been studied in order to determine the principles upon which the design of efficient interrogation algorithms rests. These principles are summarized in the first section of this Appendix and are then employed to derive a scheduling algorithm for the representative CAST system presented in Section 1.4.

E.1 THE INTERROGATION SCHEDULING PROBLEM

The function of interrogation scheduling in CAST is to ensure that transmissions from different aircraft do not overlap at any of the receiver satellites. Scheduling algorithms can be judged by two criteria; their efficiency of channel usage and the computation required to execute the algorithm. Our discussion in this appendix addresses only the efficiency issue, and emphasizes the maximization of efficiency, since this tends to maximize the system capacity.

Ideally, an interrogation schedule operates by specifying a transmission time for each aircraft based upon the current positions of all aircraft and all satellites. However, this ideal basis for scheduling is compromised by certain features of the system. Among those features are the following two which are given specific treatment in the sequel.

1. The times at which aircraft can transmit are restricted somewhat by the finite duration of the interrogation signal, the serial interrogation procedure within a given satellite beam, and the dual function of the interrogator satellite as a receiver.

2. The positions of the aircraft are not precisely known at the time of interrogation; thus the system is required to function on the past history of the aircraft tracks, which are themselves subject to measurement error.

In order to understand how an interrogation schedule might be determined, let us consider the problem of the successive interrogation of two aircraft. Figure E.1 shows two aircraft separated by a distance d, and at and inclination angle of ϕ relative to the tangent plane of the earth below. The interrogator satellite appears at elevation and azimuth angles θ_i and θ_a, respectively.* We also define the following parameters:

τ_i = duration of interrogation signal

τ_r = duration of reply signal

θ_r = minimum elevation angle of any receiver satellite.**

It can be shown that the amount of dead time, τ_d, which is inserted between the termination of interrogation 1 and the beginning of interrogation 2 (the interrogations are increasing range ordered from the satellite) in order to ensure that the two replies do not overlap at any receiver satellite, must satisfy

*Azimuth is measured relative to the plane which contains the two aircraft and is normal to the earth's tangent plane.

**Note that $\theta_r \leq \theta_i$, since the interrogator is also a receiver.

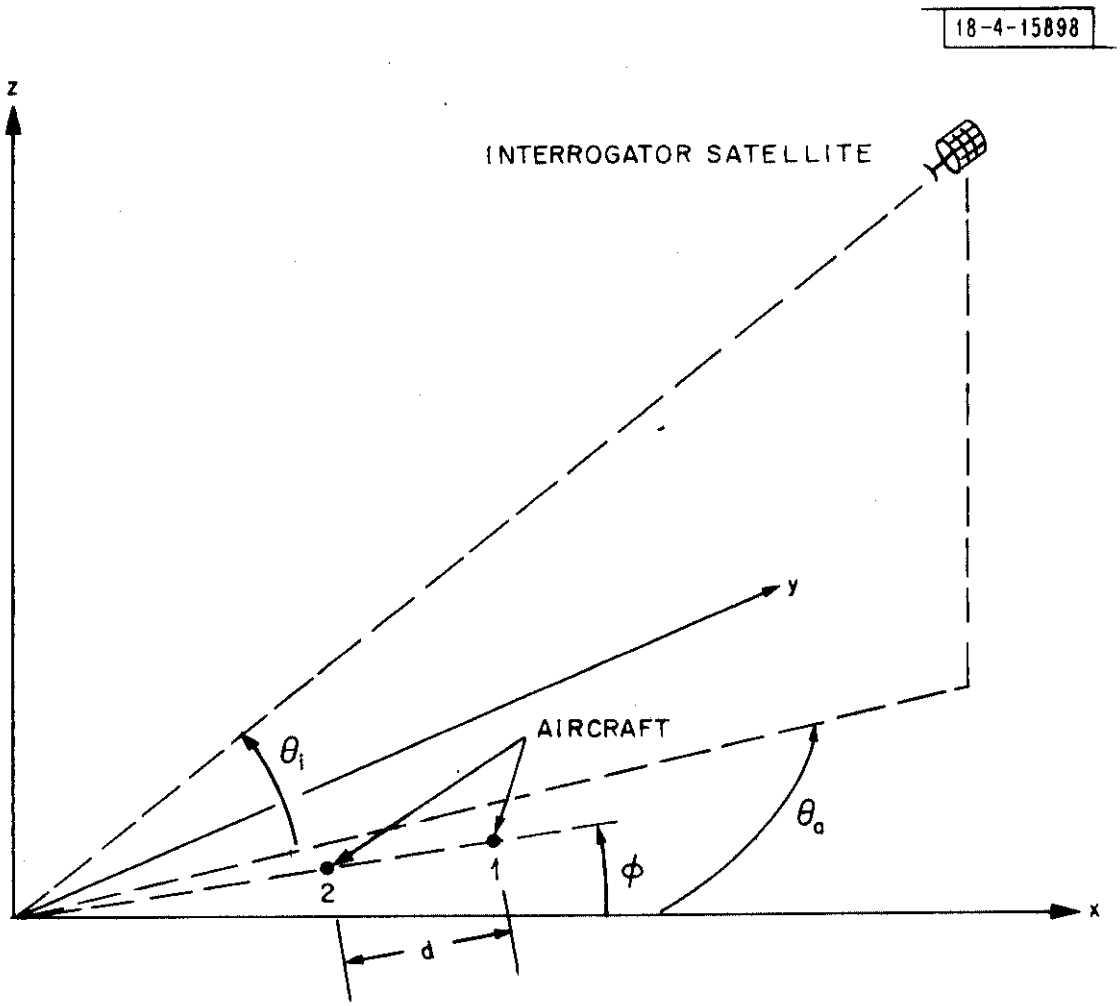

Figure E.1. Geometry of Successively Interrogated Aircraft Positions and Interrogator Satellite.

$$\tau_d \geq \max\{0,\ (\tau_r - \tau_i) + (d/c)[\cos(\theta_r - \phi) - \cos\theta_a \cos\theta_i \cos\phi - \sin\theta_i \sin\phi]\}$$

(E-1)

where c = speed of light.

A number of immediate implications can be drawn from (E-1). One can determine that the following circumstances tend to minimize the required dead time:

1. Replies short compared to interrogations
2. Low interrogation elevations
3. High receiver elevations (small satellite cone high angles)
4. Small interrogation azimuth offsets (θ_a)
5. Small aircraft spacing
6. Decreasing altitude of successively interrogated aircraft.

Unfortunately, a number of these circumstances are either mutually inconsistent or conflict with other objectives. Nevertheless, some rather useful preliminary conclusions can be drawn from this result. Efficient use of the channel is made by interrogating from a satellite which is at low elevation; successively interrogated aircraft should be close together, increasing range-ordered from the satellite and chosen so that their ground positions and the interrogator subsatellite position* are essentially colinear.**

*The subsatellite position is the point at which the straight line connecting the interrogator and the center of the earth intersects the surface of earth.

**Colinearity is defined relative to great circles on the earth.

The latter finding suggests that aircraft be successively interrogated along certain straight lines in the airspace.

An algorithm in which aircraft are interrogated along thin horizontal cylinders within the airspace has been developed. In this algorithm the actual aircraft positions are replaced by virtual positions which are the projections of the actual positions onto the center line of the cylinder. Aircraft are interrogated within the cylinder according to increasing range order of virtual position. Dead time is inserted to account for altitude variations within the cylinder.

The airspace covered by each antenna beam is partitioned into rectangular solids of height h, and width w and length L, each of which is interrogated successively. In order to choose an acceptable value of τ_d, a value for the maximum allowable spacing, d, between successively interrogated aircraft must be set. The value of τ_d corresponding to the choice of d (and the other parameters) is adequate only for exactly known aircraft positions. Motion between update periods (successive roll calls) is taken into account by successively interrogating aircraft which would not be separated by more than d even if they underwent maximum velocity (V_{max}) opposite motion since their last position updates.

E.2 SAMPLE INTERROGATION ALGORITHM

Features of the algorithm apart from those discussed in Section E.1 are best brought out in the course of an example. The following algorithm illustrates an application of the techniques developed as a consequence of (E-1).

In Figure E. 2 it is assumed that CONUS is covered by a rectangle measuring 3 kmi x 1. 5 kmi. Each of 10 beams covers a 600 mi x 750 mi sector. The airspace of interest will be assumed to extend to 20, 000 ft. The following parameter values characterize the model:

$\theta_{i\ min} = 45^{o}$

$\theta_{i\ max} = 60^{o}$

$\theta_{r\ min} = 45^{o}$

$\theta_{a\ max} = 15^{o}$

$d = 10$ mi

$h = 3.79$ mi

$L = 600$ mi

$w = 5$ mi

$\tau_{i} = 180$ mi

$\tau_{r} = 200\ \mu$sec

PIAC* $= 3 \times 10^{4}$ aircraft

$V_{max} = 600$ mph

$B = 10$ total beams

$b = 5$ simultaneous beams

$\alpha = 10$ sec roll call period

Most of the assumptions in the above list are based on the results of Sections 5 and 6 of this report. The assumptions about interrogator satellite positions (elevation and azimuth motions) are based on preliminary results of constellation studies [13].

*PIAC = Peak Instantaneous Airborne Count

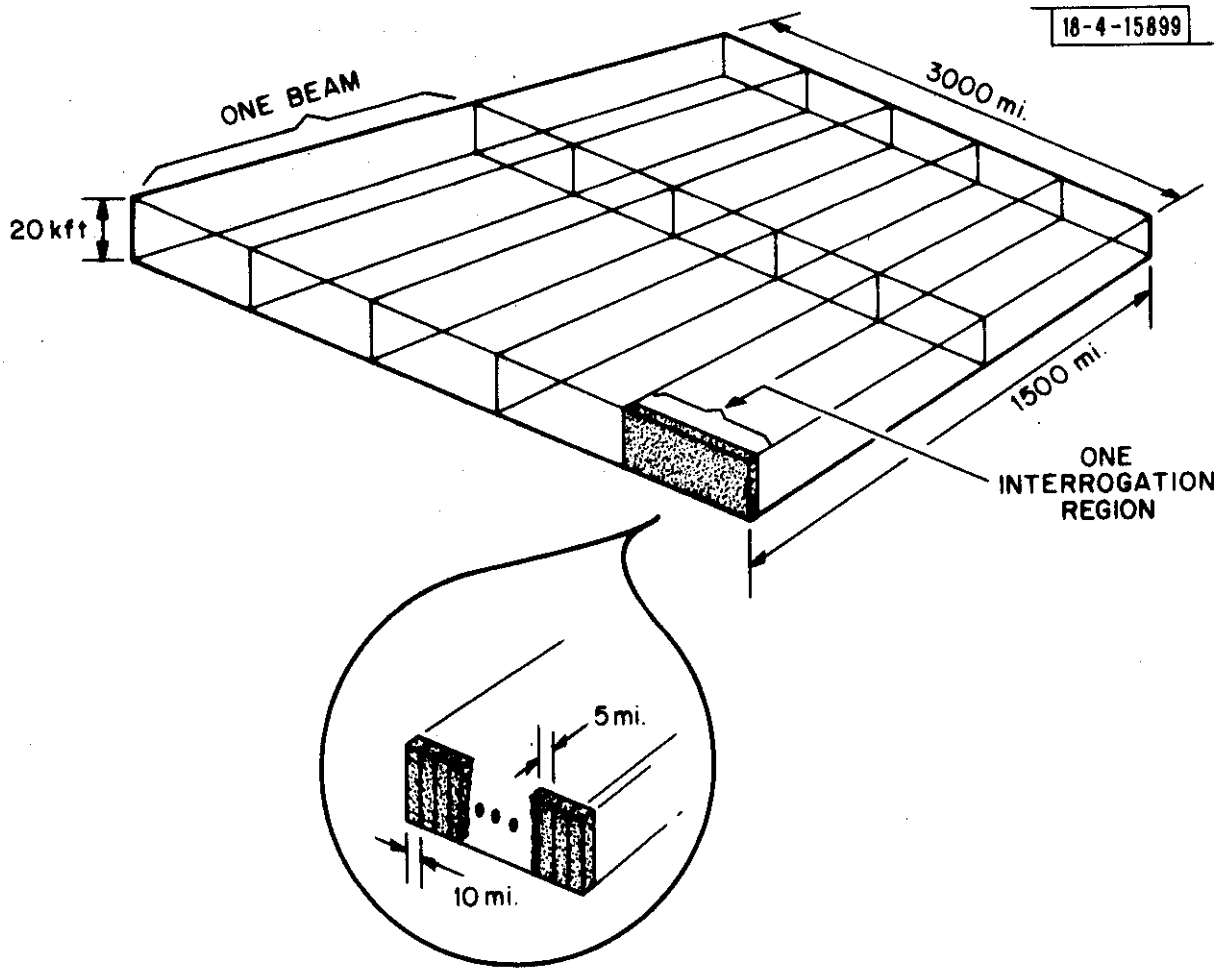

Figure E. 2. Decomposition of CONUS Airspace Into Beams and Interrogation Regions.

We now define

τ_1 = dead time between successive interrogations.

The dead time τ_1 has several components. The first, τ_{11}, is dead time required between successive interrogation of virtual positions:

$$\tau_{11} = (200 - 180)\ \mu\text{sec} + \frac{10 \text{ mi}}{1.86 \times 10^5 \text{ mi/sec}} [\cos 45^\circ - \cos 60^\circ \cos 15^\circ] \qquad \text{(E-2)}$$

$$= 32\ \mu\text{sec} \quad .$$

The second accounts for altitude variation:

$$\tau_{12} = \sqrt{\frac{(3.79)^2 + (5)^2 \text{ mi}}{1.86 \times 10^5 \text{ mi/sec}}} \quad (\sin 45^\circ + \sin 60^\circ)$$

$$= 53\ \mu\text{sec} \quad . \qquad \text{(E-3)}$$

This latter delay is large and indicates that perhaps w was poorly chosen; a value $w \simeq h$ might be more appropriate.

The third component is the relative motion delay. If two aircraft are within 10 miles of one another at one instant, they can be separated by no more than 13.33 (=10 + 2 x 0.167/sec x 10 sec) miles after the passage of

10 seconds. The dead time τ_{11} can then be incremented as though it were originally computed for an effective center line separation d' = 13.33 miles:

$$\tau'_{11} = (200 - 180)\ \mu\text{sec} + \frac{13.33\ \text{mi}}{1.86 \times 10^5\ \text{mi/sec}} (\cos 45^\circ - \cos 60^\circ \cos 15^\circ)$$

$$= 36\ \mu\text{sec} \quad . \tag{E-4}$$

The total time per interrogation is thus

$$T_i = \tau_i + \tau'_{11} + \tau_{12} = (180 + 36 + 53)\ \mu\text{sec}$$

$$= 269\ \mu\text{sec} \quad . \tag{E-5}$$

The expected number of aircraft within a 600 mi x 5 mi x 20 kft sector is 20, so that the expected time to interrogate the region is*

$$T_{\text{region}} = 20 \times 269\ \mu\text{sec} = 5.38\ \text{msec} \quad . \tag{E-6}$$

After the interrogation of a rectangular solid region, delay τ_2 must be inserted before interrogation of a new region begins. The required delay can be computed from a formula similar to (E-1):

*This assumes that an aircraft is available to be interrogated every 250 μsec. A model can be developed to cover the situation in which this is not the case.

$$\tau_2 = \frac{600 \text{ mi}}{1.86 \times 10^5 \text{ mi/sec}} (\cos 45^\circ + \cos 60^\circ \cos 15^\circ)$$

$$= 3.84 \text{ msec} \quad . \tag{E-7}$$

A single beam contains 150 such regions and is interrogated in

$$T_{beam} = 150 (T_{region} + \tau_2)$$

$$= 1.38 \text{ } \mu\text{sec} \quad . \tag{E-8}$$

We can see that the interrogation of a single beam cannot proceed uninterrupted, because the round trip time to a synchronous satellite is only a few hundred msec. The transmit-receive duty cycle will be essentially 50% since the span of a single beam (~600 mi) is small relative to the interrogating satellite distance. A reasonable procedure, depending on the constellation geometry, might be to interrogate 10 adjacent regions, which would occupy 88.4 (= 10 x 5.38 + 9 x 3.84) msec, and to receive for a similar length of time. Interrogation of the full beam requires 15 iterations of this procedure. In this case, the beam is interrogated in

$$T_{beam} = 15 \times 2 \times 88.4 \text{ msec}$$

$$= 2.65 \text{ sec} \quad . \tag{E-9}$$

Two beam cycles are required to interrogate all of CONUS; the required interrogation period, α, is at least 5.3 sec. This is smaller than the 10 second period previously assumed. At this rate the system could handle about 56,000 aircraft in 10 seconds.

For the above system, the transmitter is on for a total of

$$T_{on} = 2 \text{ beams} \times 3 \times 10^3/\text{beam} \times 180\ \mu\text{sec}$$

$$= 1.1 \text{ sec} \qquad \text{(E-10)}$$

so that the efficiency is

$$\eta = \frac{T_{on}}{\alpha} = \frac{1.1}{5.3} = 20.8\% \quad . \qquad \text{(E-11)}$$

REFERENCES

[1] "Final Report - Advanced Air Traffic Management System," Report C72-1206/201. Rockwell International Corporation, Anaheim, California (April 1973).

[2] L. Schuchman, "The ASTRO-DABS Concept," Technical Report MTR-6287, MITRE Corporation, McLean, Virginia (November 1972).

[3] "Advanced Air Traffic Management - System B Summary Report," MTR-6419 Series 1, MITRE Corporation, McLean, Virginia (June 1973), FAA-EM-73-10.

[4] "Study and Concept Formulation of a Fourth Generation Air Traffic Control System," Vols. I-V, Report DOT-TSC-3601-1, Boeing Company, Renton, Washington (April 1972).

[5] P.M. Diamond, "The Potential of a System of Satellites as a Part of an Air Traffic Control System," AGARD Conference Proceedings No. 105, p. 20-1 (June 1972).

[6] D.D. Otten, "Study of a Navigation and Traffic Control Technique Employing Satellites," Vols. I-IV, Group Report 08710-6012-12000, TRW Systems, Redondo Beach, California (December 1967).

[7] K.D. McDonald, "A Survey of Satellite-Based Systems for Navigation, Position Surveillance, Traffic Control and Collision Avoidance," Addendum to Proceedings of ION National Aerospace Meeting, Institute of Navigation, Washington, D.C. (March 1973).

[8] K.S. Schneider and R.S. Orr, "Technical Assessment of Satellites for CONUS Air Traffic Control, Vol. II: Random Access Aircraft-to-Satellite Techniques," Project Report ATC-26, Lincoln Laboratory, M.I.T. (to be published).

[9] H.B. Lee and B.B. Goode, "Technical Assessment of Satellites for CONUS Air Traffic Control, Vol. III: Satellite-to-Aircraft Techniques," Project Report ATC-26, Lincoln Laboratory, M.I.T. (to be published).

[10] K.S. Schneider, I.G. Stiglitz and A.E. Eckberg, "Surveillance Aspects of the Advanced Air Traffic Management System," Project Report ATC-10, Lincoln Laboratory, M.I.T. (22 June 1972), DOT/TSC-241-2.

[11] E.J. Kelly, "The Use of Supplementary Receivers for Enhanced Positional Accuracy in the DAB System," Technical Note 1972-28, Lincoln Laboratory, M.I.T. (4 December 1972).

[12] B.D. Elrod, "Aircraft Interrogation Scheduling with ASTRO-DABS," Technical Report MTR-6368, MITRE Corporation, McLean, Virginia (March 1973).

[13] H.B. Lee and A.E. Wade, "Improved Satellite Constellations for CONUS ATC Coverage," Project Report ATC-23, Lincoln Laboratory, M.I.T. (to be published).

[14] H.L. Gerwin and G.K. Campbell, "The Wrap Rib Parabolic Reflector Antenna," Report LMSC/A969503, Lockheed Missiles and Space Company, Sunnyvale, California.

[15] I.G. Stiglitz, J.U. Beusch, A. Eckberg, K.S. Schneider, "Concept Formulation Studies of the Surveillance Aspects of the Fourth Generation Air Traffic Control System," Project Report ATC-7, Lincoln Laboratory, M.I.T. (21 September 1971).

[16] G.V. Colby and E.A Crocker, "Final Report Transponder Test Program," Project Report ATC-9, Lincoln Laboratory, M.I.T. (12 April 1972), FAA-RD-72-30.

[17] G.V. Colby and E.A. Crocker, "Transponder Frequency Drift During a 100 Microsecond Pulse Transmission," private communication.

[18] G. Ploussios, "Noise Temperature of Airborne Antennas at UHF," Technical Note 1966-59, Lincoln Laboratory, M.I.T. (6 December 1966), DDC AD 644 829.

[19] "Development of a Discrete Address Beacon System," Quarterly Technical Summary, Lincoln Laboratory, M.I.T. (1 January 1973), pp. 7-9, FAA-RD-73-12.

[20] "Report of the DOT Air Traffic Control Advisory Committee," DOT (December 1969), U.S. Govt. Printing Office 1970 O-375-448.

[21] H.L. Van Trees, Detection, Estimation, and Modulation Theory Part I (Wiley, New York, 1968).

[22] R.S. Orr and R.D. Yates, "On the Estimation of the Arrival Time of Pulse Signals in Gaussian Noise," Technical Note, Lincoln Laboratory, M.I.T. (to be published).

[23] P. Swerling, "Parameter Estimation For Waveforms In Additive Gaussian Noise," J. Soc. Indust. Appl. Math., Vol. 7, No. 2, pp. 152-166 (June 1959).

[24] L. P. Seidman, "An Upper Bound on Average Estimation Error in Non-linear Systems," IEEE Trans. Info. Thy. IT-14, pp. 243-250 (March 1968).

[25] D. F. Delong, "Experimental Autocorrelation of Binary Codes," Group Report 47G-0006, Lincoln Laboratory, M. I. T. (24 October 1960), DDC-245803.

[26] N. N. Rao, M. Y. Youakim and K. C. Yeh, "Feasibility Study of Correcting for the Excess Time Delay of Transionospheric Navigational Ranging Signals," Technical Report 43, U. Illinois Ionosphere Radio Laboratory (July 1971), SAMSO TR71-163.

[27] B. B. Goode, private communication.

[28] W. W. Peterson and E. J. Weldon, Error Correcting Codes, Second Edition, (M. I. T. Press, Cambridge, 1972).

[29] H. B. Lee, "Accuracy Limitations of Hyperbolic Multilateration Systems," Technical Note 1973-11, Lincoln Laboratory, M. I. T. (22 March 1973), DOT/TSC-241-3.

ACKNOWLEDGEMENTS

The authors gratefully acknowledge G. V. Colby, P. H. Robeck and J. D. Welch for their assistance in understanding the issues concerning general aviation avionics. Dr. R. D. Yates assisted in developing time of arrival estimation bounds and Dr. B. B. Goode provided informative data concerning ionospheric delays and satellite tracking errors. Dr. A. E. Eckberg performed the original work on interrogation algorithms upon which many of our results are based. Drs. T. J. Goblick and W. H. Harman carefully proof-read the final draft of this document. Finally, the authors thank Dr. I. G. Stiglitz for providing the overall direction to our efforts.